Annu. Rev. Astron. Astrophys. 1994. 32: 419–63

COSMIC DUSTY PLASMA

D. A. Mendis and M. Rosenberg

Department of Electrical and Computer Engineering, University of California, San Diego, La Jolla, California 92093

KEY WORDS: dust-plasma interactions, charged dust, collective processes

1. INTRODUCTION

Different types of photometric observations in the 1930s (Trumpler 1930; Stebbins et al 1934; 1939) clearly showed that the dark "holes" in the Milky Way, observed by William Herschel almost 150 years earlier, were in fact regions of heavy obscuration by cosmic dust. Continuing observations since then have established that dust is an almost ubiquitous component of the cosmic environment. Remote sensing of dust in the interstellar, circumstellar, interplanetary, circumplanetary, and cometary environments has, more recently been complemented by in-situ detections of the last three. Furthermore, the inference of the existence of very small grains (so-called VSGs with dimensions of 10–100 Å) in the interstellar medium (Puget & Léger 1989) as well as their in-situ detection in the environment of comet P/Halley (Sagdeev et al 1989) reinforces the reasonable expectation that the transition from gas to large dust particles in the cosmic environment is a continuous one through macromolecules, clusters, and VSGs.

These dust grains are invariably immersed in ambient plasma and radiative environments. They must therefore be necessarily electrically charged and consequently coupled to the plasma through electric and magnetic fields, with the coupling becoming stronger as the grain size decreases.

While any plasma containing such charged dust grains is often loosely referred to as a dusty plasma, there are different regimes characterized by the relative magnitudes of three characteristic length scales, namely the dust grain size a, the plasma Debye length λ_D, and the average intergrain distance $d(\approx n_d^{-1/3}$, where n_d is the dust number density). In general cosmic plasma environments that are contaminated by dust can be characterized by either of two conditions 1. $a \ll \lambda_D < d$ or 2. $a \ll d < \lambda_D$. In the first case the dust may

0066–4146/94/0915–0419$05.00

Table 1 d/λ_D for a few cosmic environments

	$n_i(cm^{-3})$	$T(°K)$	$n_d(cm^{-3})$	d/λ_D	$a(\mu m)$
Interstellar clouds[a]	10^{-3}	10	10^{-7}	0.3	0.01–10
Noctilucent clouds[a]	10^3	150	10	0.2	~1
Saturn's E-ring[b]	10	10^5–10^6	10^{-7}–10^{-8}	$\lesssim$1	~1
Halley's Comet					
1. inside ionopause[c]	10^3–10^4	$< 10^3$	10^{-3}	$\gtrsim$1	.1~10
2. outside ionopause[d]	10^2–10^3	$\sim 10^4$	5×10^{-9}–10^{-7}	$\gtrsim$10	.01~10
Saturn's spokes[b]	0.1–10^2	2×10^4	1	$\lesssim$0.01	$\lesssim$1
Saturn's F-ring[b]	10–10^2	10^5–10^6	<30	$\lesssim 10^{-3}$	$\lesssim$1

[a]Tsytovich et al (1990), [b]Goertz (1989), [c]Mendis et al (1985), [d]De Angelis et al (1988).

be considered as a collection of isolated screened grains ("dust-in-plasma"); in the second case the dust also participates in the screening process and therefore in the collective behavior of the ensemble (a true "dusty-plasma"). Estimates of the ratio d/λ_D in a few cosmic environments are shown in Table 1.

That cosmic dust would be electrically charged has been recognized for a long time (Spitzer 1941), yet theoretical studies of its many consequences was slow in coming. A strong impetus for the study of dust-plasma interactions in space came with the observations of curious features like the "radial spokes" across Saturn's B Ring by the *Voyager* spacecraft's cameras in the early 1980s (e.g. Hill & Mendis 1982a, Goertz & Morfill 1983). Presently, theoretical studies of cosmic dust-in-plasmas as well as dusty plasmas are proceeding at a rapidly increasing pace and dedicated laboratory studies, while lagging behind the theory, are beginning to make significant contributions in checking the predictions of various theories.

Several useful reviews of the present subject have appeared recently (Goertz 1989, Hartquist et al 1992, Northrop, 1992). The present review, in common with all of the above, does not pretend to be comprehensive. Rather than focusing on individual phenomena, we attempt to emphasize the basic physics that underlie both dust-in-plasma and dusty plasmas in space. We hope that this rather theoretical approach will prove useful to both the interested outsider as well as to a graduate research student who might contemplate entering this emerging new field.

We start (in Section 2) with a detailed discussion of the problem central to all the subsequent studies, which is the electrostatic charging of dust grains both when they may be regarded as being "isolated" and when they form an interacting ensemble. This is followed, in Section 3, with some of the physical consequences to the dust, such as electrostatic disruption, coagulation, and levitation. In Section 4, we consider the dynamics and orbital evolution of charged dust in cosmic environments where long-range intergrain electrical in-

teractions are unimportant. In Section 5 we discuss the collective behaviors that are manifested: waves and instabilities. Here we distinguish between the cases in which the charged dust is considered to be massive and immobile and in which dust dynamics plays a role in wave behavior. We also discuss the role of charged dust in wave scattering.

2. ELECTROSTATIC CHARGING OF THE DUST

Central to all the studies that are discussed is the charge Q acquired by the dust grains. For a given dust grain at a given time, this is determined by the equation

$$\frac{dQ}{dt} = \frac{d}{dt} \cdot C(\phi - \overline{\phi}) = I, \tag{1}$$

where I is the total current to the grain, C is the grain capacitance, ϕ is the grain surface potential, and $\overline{\phi}$ is the average potential of the ambient plasma with a dust grain distribution. Contributions to I come from various electron and ion currents (see e.g. Whipple 1965) and include (*a*) electron and ion collection, (*b*) photo emission, (*c*) secondary electron emission due to energetic electron impact, (*d*) secondary electron emission due to energetic ion impact, (*e*) electric field emission, (*f*) thermoionic emission, (*g*) triboelectric emission, and (*h*) radioactive emission of electrons and α particles.

Of these, the most important in the cosmic environment are in general (*a*), (*b*), and (*c*), while (*e*) is important for very small grains. Friction-mediated (triboelectric) emission is known to be important in the charging of dust in volcanic plumes, and may also have played some role in the early protoplanetary nebula.

The currents to the grains depend on a number of properties of both the grains and the ambient medium. For instance, the electron and ion collection currents depend not only on the size and shape of the grains, but also on the electron and ion velocity distributions and densities, motion of the grain relative to the plasma, and the potential difference between the grain surface and the ambient dusty plasma, $(\phi_s - \overline{\phi})$. The photo-electron current depends on the electric properties of the grain, the grain surface potential, and of course, on the photo ionizing (uv) flux of radiation. The secondary electron emission current due to energetic electron impact depends on the secondary emission yield, which has recently been shown to be crucially dependent on the grain size (Chow et al 1993). The electric field emission current, which is caused by large surface electric fields, is negligible for the larger grains, but could become the dominant one when the grains become very small (Mendis & Axford 1974).

In a steady state, the grains may reach an equilibrium surface potential, ϕ_s, with respect to the plasma. Then $\frac{dQ}{dt} = 0$ and $Q = C(\phi_s - \overline{\phi})$. The values of both C and $\overline{\phi}$ depend on how closely the grains are packed together. For instance when $d \gg \lambda_D$, the grains may be regarded as being isolated. Then $C = C_{\text{iso}} = a(1 + a/\lambda_D)$ and $\overline{\phi}$ may be taken to be zero. On the other

hand, when $d \ll \lambda_D$, C increases slightly above $C_{\rm iso}$ but $\overline{\phi}$ approaches ϕ_s and consequently the grain charge becomes very much smaller than $Q_{\rm iso}$ (Goertz & Ip 1984, Whipple et al 1985).

2.1 *Isolated Grain*

In order to illustrate some of these points, let us start with the simplest case of a small "isolated" ($a \ll \lambda_D \ll d$) grain at rest with respect to the plasma, and assume that the only currents of importance are electron and ion collection.

If $f_{\rm e}(E)$ is the isotropic electron velocity distribution at infinity, where E is the kinetic energy ($= \frac{1}{2}m_e v_e^2$), the electron current (density) to the grain is given by

$$J_{\rm e} = -e \iiint f_e(E - e\phi_{\rm s}) v_n d^3\mathbf{v}. \tag{2}$$

Here v_n is the component of the velocity normal to the grain surface, and the integration is performed over all orbits that intersect the grain, i.e. for $E_{\rm total} = E - e\phi_{\rm s} \geq 0$. (e.g. see Laframboise & Parker 1973). Selecting spherical polar coordinates so that $d^3\mathbf{v} = v^2 \sin\theta \, d\theta \, d\phi \, dv$ and integrating over θ and ϕ one easily obtains

$$J_{\rm e} = -\frac{2\pi e}{m_{\rm e}^2} \int_{\max(0, e\phi_{\rm s})}^{\infty} E f_{\rm e}(E - e\phi_{\rm s}) \, dE. \tag{3}$$

Similarly, the ion current density to the grain is

$$J_{\rm i} = +\frac{2\pi e}{m_{\rm i}^2} \int_{\max(0, e\phi_{\rm s})}^{\infty} E f_i(E + e\phi_{\rm s}) dE. \tag{4}$$

The forms of $J_{\rm e,i}$ when f is Maxwellian are well known (e.g. see Goertz 1989). The equilibrium potential, obtained by equating the total current density $J_{\rm e} + J_{\rm i}$ to zero, in that case, is given by the well-known transcendental equation

$$\left(\frac{m_{\rm i}}{m_{\rm e}}\right)^{1/2} = R_T^{1/2} \left(1 - \frac{e\phi_{\rm s}}{k_{\rm B} T_{\rm i}}\right) \exp\left(-R_T \frac{e\phi_s}{k_{\rm B} T_{\rm i}}\right), \tag{5}$$

where $R_T = T_{\rm i}/T_{\rm e}$.

If we also assume that the plasma consists of electrons and protons and further that $T_{\rm e} = T_{\rm i} = T$, the solution of Equation (5) gives $\phi_{\rm s} \approx -2.51 \, k_{\rm B} T/e$. The equilibrium potential is negative, in this case, because initially (i.e. when $\phi_{\rm s} = 0$) more electrons (whose mobility is about 43 times that of the protons when $T_{\rm e} = T_{\rm i}$) than protons reach the grain surface and charge it negative. This causes the electron current to decrease and the ion current to increase, thereby increasing the grain potential, and the process will proceed until the grain acquires the equilibrium negative potential $\phi_{\rm s}$ that makes these two currents equal in magnitude. For an electron-oxygen ion plasma the equilibrium potential $\phi_{\rm s}$

is more negative ($\approx -3.6k_BT/e$) owing to the even smaller mobility of the heavier oxygen ions.

Astrophysical calculations generally assume that the plasma is indeed Maxwellian, a notable exception being that of Meyer-Vernet (1982), which includes suprathermal electrons. Most astrophysical plasmas, however, are observed to have non-Maxwellian high energy tails (e.g. Summers & Thorne 1991), and a generalized Lorenzian (κ) distribution has been often employed to fit the observed particle distributions (Gosling et al 1981, Leubner 1982, Armstrong et al 1983, Christon et al 1988). Consequently it is instructive to use such a distribution to recalculate the potential of an isolated small grain, as was done recently by Rosenberg & Mendis (1992). The normalized κ-distribution is given by

$$f_\kappa(E) = n\left(\frac{m}{2\pi\kappa E_0}\right)^{3/2}\frac{\Gamma(\kappa+1)}{\Gamma(\kappa-1/2)}\cdot\left(1+\frac{E}{\kappa E_0}\right)^{-(\kappa+1)} \tag{6}$$

where κ is the spectral index, E is the particle energy, n is the particle number density, Γ is the gamma function, and E_0 is related to the temperature T by $E_0 = [(2\kappa-3)/2\kappa]k_BT$ for $\kappa > 3/2$. This distribution is also ideal for studying how the grain potential responds to increasing deviation from the Maxwellian plasma, because while it has a high energy tail with a power-law dependence $f_\kappa \propto E^{-(\kappa+1)}$ for $E \gg \kappa E_0$, it approaches the Maxwellian distribution as $\kappa \to \infty$. Following the same procedure as for a Maxwellian, described above, the equilibrium potential of the grain is now given by the equation

$$\left(\frac{m_i}{m_e}\right)^{1/2} = R_T^{1/2}(\kappa-1)\left(\frac{2}{2\kappa-3}\right)^{\kappa}\left[\frac{2\kappa-3}{2\kappa-2}-\frac{e\phi_s}{k_BT_i}\right] \times\left[\frac{2\kappa-3}{2}-R_T\frac{e\phi_s}{k_BT_i}\right]^{\kappa-1}, \tag{7}$$

where it is assumed that $\kappa_e = \kappa_i = \kappa$. This result reduces to the Maxwellian result when $\kappa \to \infty$. Equation (7) also has a particularly simple solution when $\kappa = 2$ and $R_T = 1$, e.g.

$$\frac{e\phi_s}{k_BT_i} = \frac{1}{2}\left[1-\left(\frac{m_i}{m_e}\right)^{1/4}\right]. \tag{8}$$

Although the grain potential ϕ_s is once again negative, its magnitude is found to be large as long as the electrons are described by a κ-distribution with this magnitude increasing with ion mass and decreasing with electron κ (see Figure 1). For example, for a pure oxygen Maxwellian plasma (with $T_e = T_i = T$), $\phi_s \simeq -3.6k_BT/e$, as stated earlier, whereas $\phi_s \approx -6.1k_BT/e$ when $\kappa_e = \kappa_i = \kappa = 2$ and $\phi_s \approx -4.5k_BT/e$ when $\kappa_e = \kappa_i = \kappa = 5$. This last case with $\kappa = 5$ is the one that appears to best describe space plasmas in several instances. The

consequences of this increase in the magnitude of the grain potential will be discussed later.

So far we have assumed that the grain is at rest with respect to the plasma. However, grains (e.g. those in planetary rings) drift with respect to the plasma. The appropriate velocity distributions to be used in the calculation of the ion and electron collection currents are those in the frame of reference of the moving grain. Since drift speeds of these grains are very much smaller than the electron thermal speeds in the region of the planetary rings (e.g. Mendis et al 1984), they have negligible effect on the electron current. On the other hand, they are of the same order as the ion thermal speeds, so the ion current is strongly modified. The modified ion current for the case of a drifting Maxwellian in the grain frame is given in Whipple (1965, 1981). It was often assumed in the literature that this effect increases the ion current since one expects the moving grain to sweep up more ions. This in turn would make the grain potentials

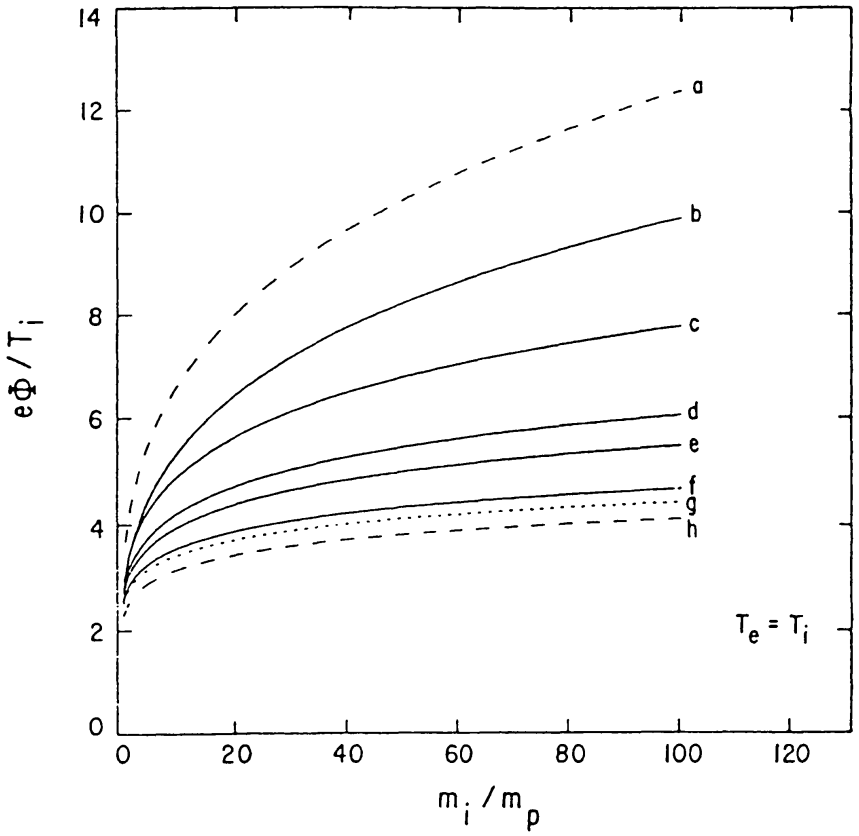

Figure 1 Plot of $e\Phi/T_i(\Phi = |\phi|, \phi < 0)$ as a function of ion mass (normalized to the proton mass) for $T_e = T_i$ in a Lorentzian plasma. The labels attached to the curves refer to the following spectral indices: (*a*) $\kappa_e = 2$, Maxwellian ions ($\kappa_i \to \infty$); (*b*) ($\kappa_e = \kappa_i = 2$; (*c*) $\kappa_e = \kappa_i = 3$; (*d*) $\kappa_e = \kappa_i = 5$; (*e*) $\kappa_e = \kappa_i = 7$; (*f*) $\kappa_e = \kappa_i = 25$; (*g*) Maxwellian electrons and ions ($\kappa_e = \kappa_i \to \infty$); and (*h*) $\kappa_i = 2$, Maxwellian electrons ($\kappa_e \to \infty$). Note that T_i is in energy units. (From Rosenberg & Mendis 1992.)

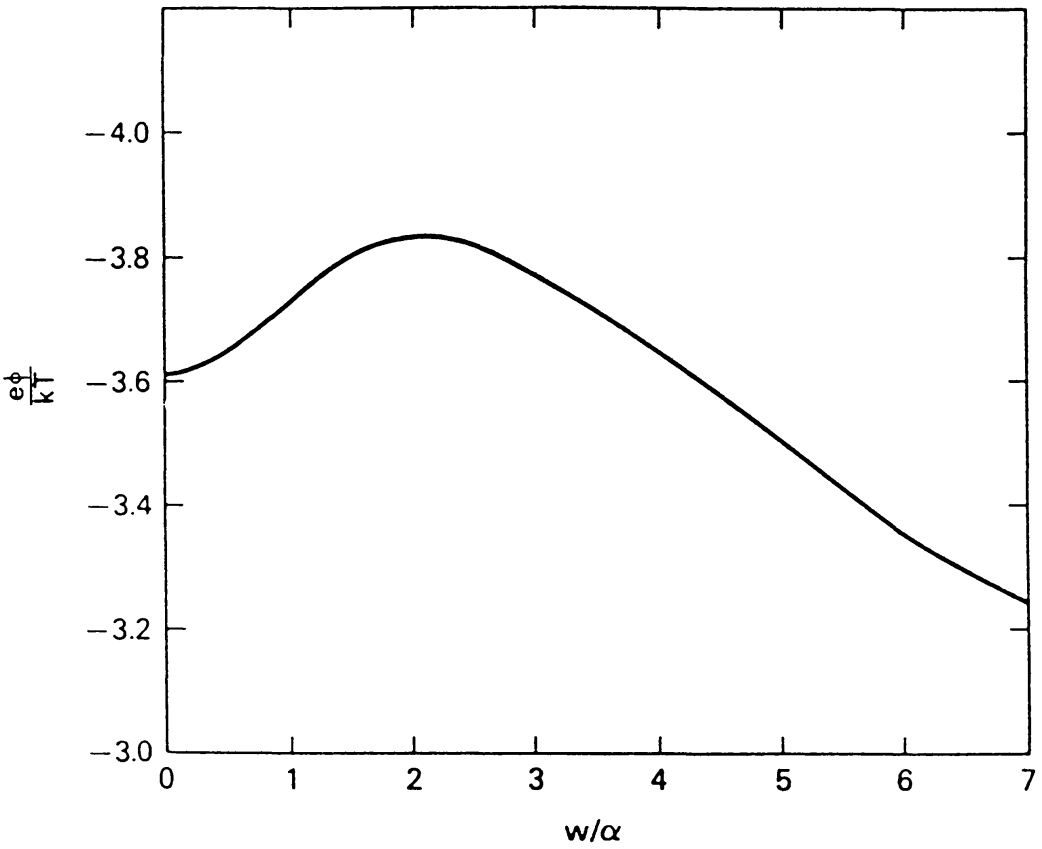

Figure 2 Normalized grain potential as a function of the ratio of the grain velocity w to the ion thermal velocity. (From Northrop et al 1989.)

less negative. A more recent study (Northrop et al 1989) has shown this to be so only when the Mach number M (grain speed/ion thermal speed) $\gtrsim 2$ (see Figure 2). When $0 < M \lesssim 2$ the grain potential turns out to be more negative. The reason for this is that the increase of ion flux on the leading face of the grain is more than offset by its decrease on the trailing face for this range of values of M. This is not the case when $M \gtrsim 2$.

A dominant process associated with grain charging at higher electron energies ($\gtrsim 50$ eV) is secondary electron emission, and such electron energies are common in certain regions of planetary magnetospheres. In this process, energetic electrons penetrate the grain and energize material electrons that may diffuse out of the grain. One defines the secondary electron yield $\delta(E)$, at a given energy E of the primary electrons, as the ratio of the secondary electron current to the primary electron current. Then the secondary electron current density J_s is given by

$$J_s = \frac{2\pi e}{m_e^2} \int_0^\infty E\delta(E) f_e(E - e\phi_s)\, dE, \quad \phi_s \leq 0 \tag{9}$$

$$J_s = \frac{2\pi e}{m_e^2}\exp\left(-\frac{e\phi_s}{k_B T_s}\right)\left(1+\frac{e\phi_s}{k_B T_s}\right)\int_{e\phi}^{\infty} E\delta(E) f_e(E-e\phi_s)\,dE, \quad \phi_s \geq 0. \tag{10}$$

Here $k_B T_s$ is the thermal energy of the emitted secondary electrons (which are found to have a Maxwellian velocity distribution) with values in the range of 2–5 eV, regardless of the energy of the incoming primaries (e.g. Goertz 1989). The forms of J_s when $f_e(E)$ is either a Maxwellian or a generalized Lorentzian are given in Chow et al (1993), where the expressions for $\delta(E)$ for different grain sizes and grains materials are also calculated. Due to shape of $\delta(E)$, which first increases with energy to a maximum δ_m (which could be $\gg 1$) at some E_m, and then decreases monotonically (at least for grains typically $\gtrsim 0.1\mu$m), the current-energy curve of the grain subject only to electron and ion collection and secondary emission can have single or multiple real roots (Whipple 1965, Meyer-Vernet 1982): one negative root, and one positive root, or one negative and two positive roots, although the smaller positive root is unstable in the last case.

2.2 *Grain Ensemble*

We now consider the case of grain charging by plasma collection currents when the grain density in the plasma is high. In this case, the grain charge may be lower than its "isolated" value, as discussed earlier. There are two competing effects that lead to this result; one is that the capacitance of the grain increases, which tends to increase the charge, and the other is that the magnitude of the grain surface potential relative to the plasma potential decreases, which decreases the charge. The capacitance of a grain increases from its value in vacuum (where the capacitance is proportional to the grain radius) as the grain spacing becomes comparable to or less than the Debye length. In this case, the positive sheath (for a negatively charged grain) moves closer to the grain surface, thus essentially decreasing the capacitor gap, or the distance between the edge of the sheath and the grain surface, thereby increasing the capacitance (Whipple et al 1985, Northrop 1992). This effect, however, was found to be of the order of $< 0.1\%$ for parameters representative of the F Ring and the spokes of Saturn's ring system (Whipple et al 1985), where the dust density has been inferred to be comparable to the plasma density (e.g. Goertz 1989).

The more important effect at high dust density arises from electron depletion, when the dust grains carry a significant fraction of the (negative) charge density in the plasma, so that much of the electron charge resides on the grain surfaces. In this case, the surface potential of a grain does not have to be as negative with respect to the plasma potential as in the isolated grain case to balance the electron and ion currents to the grain. This leads to a decrease in the magnitude of the grain charge, since the charge is proportional to $\phi_s - \overline{\phi}$. Whipple et al

(1985) analyzed this effect by balancing the electron and ion current to the grain (considering only collection currents),

$$I_e = -e\left(\frac{8\pi k_B T_e}{m_e}\right)^{1/2} a^2 \bar{n}_e \exp[e(\phi_s - \bar{\phi})/k_B T_e] \tag{11}$$

$$I_i = e\left(\frac{8\pi k_B T_i}{m_i}\right)^{1/2} a^2 \bar{n}_i [1 - e(\phi_s - \bar{\phi})/k_B T_i], \tag{12}$$

taking into account the fact that the electron and ion densities $(\bar{n}_e, \bar{n}_i)$ in the plasma reservoir between the grain satisfy the condition of overall charge neutrality in the plasma

$$\bar{n}_e - \bar{n}_i = \eta_d Q/e. \tag{13}$$

Here ϕ_s is the grain surface potential, the reservoir of plasma between the grains is at an average potential $\bar{\phi}$, $\phi_s < 0$, Q is the grain charge, and $\eta_d = n_d/(1 - 4\pi a^3 n_d/3)$ is essentially the grain density. This leads to an equation for $y = e(\phi_s - \bar{\phi})/k_B T (T_e = T_i = T)$ as a function of a parameter $Z = 4\pi\lambda_D^2 \eta_d C(n_d)$, where $C(n_d)$ is the grain capacitance, and λ_D is the Debye length in the electron-ion plasma reservoir, $\lambda_D^2 = k_B T/[4\pi(\bar{n}_e + \bar{n}_i)e^2]$:

$$(1 - y)(1 - yZ) = \left(\frac{m_i}{m_e}\right)^{1/2} (1 + yZ)\exp(y). \tag{14}$$

Figure 3 shows the solution obtained from Equation (14) where it is seen that y, which is proportional to the grain charge $Q = C(\phi_s - \bar{\phi})$, decreases steeply with increasing Z, which is proportional to the dust density. Since the quantity Z is of the order of the ratio of the charge density on n_d "isolated" grains to the available charge density in the plasma, the depletion effect should affect grain charging when $Z \geq 1$, as shown. The condition $Z \geq 1$ implies that $4\pi n_d \lambda_D^3 \geq \lambda_D/a \gg 1$ for cosmic plasmas. The quantity yZ is essentially the ratio of the charge density carried by the grains to the charge density carried by the electrons and ions in the plasma. The decrease in grain charge arising from electron depletion can be quite large for certain plasmas; for example Whipple et al (1985) estimate that for a 1 micron grain in Saturn's F-ring, the magnitude of the negative grain charge would be $\sim 2.7 \times 10^{-4}$ times its "isolated" value. The maximum electron depletion, or minimum $\bar{n}_e/\bar{n}_i$, can be obtained from Equations (11) and (12) by solving $I_e + I_i = 0$ in the limit $y \ll 1$; this yields $\bar{n}_e/\bar{n}_i \to \sqrt{m_e/m_i}$ as $y \to 0$, and thus not all the electrons can be depleted in this approximation.

Goertz (1989) investigated how the grain potential $\phi(r)$ changes when dust grains are placed closer and closer to each other. A one-dimensional Poisson equation for the potential in the vicinity of a grain in the presence of finite electron, ion, and grain charge densities was solved numerically, coupled with

an equation for electron and ion current balance to the grain (only plasma collection currents were considered). The electrons and ions were assumed to have Boltzmann distributions, while the grain spatial distribution was modeled by a number of equally spaced infinite sheets of grains. Figure 4 illustrates how the magnitude of the spatially varying potential decreases as the grains sheets are placed closer together.

Havnes et al (1987) studied the variation of the grain charge with dust density in a dust cloud embedded in a plasma, with the cloud at an average potential V_p, using coupled equations for current balance to the grain and overall charge neutrality in the cloud. The variation of the dust grain potential minus the cloud potential $U = (|\phi_s - V_p|)$ is shown in Figure 5 as a function of a parameter $P = n_d a T / n_p$ (Havnes et al 1987, Goertz 1989), where the grain radius a is in meters, T is the plasma temperature in eV and n_p is the plasma density outside the dust cloud. The grain charge is proportional to U. Again the decrease of $|U|$ with dust charge density n_d is evident from Figure 5. Values of the parameter P for various planetary rings are shown in Table 1 of the paper by Goertz (1989) to indicate where the electron depletion effect may play a significant role in determining the grain charge. Havnes et al (1990a) have also extended

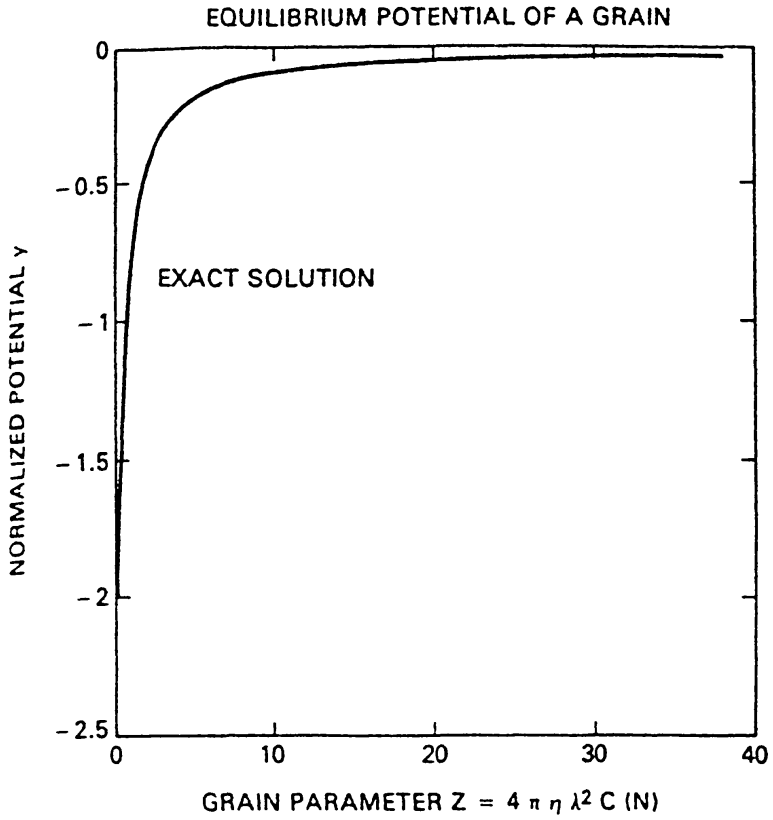

Figure 3 Dimensionless grain potential y as a function of the dimensionless parameter Z, which is quite closely proportional to the number density N of dust grains. (From Whipple et al 1985.)

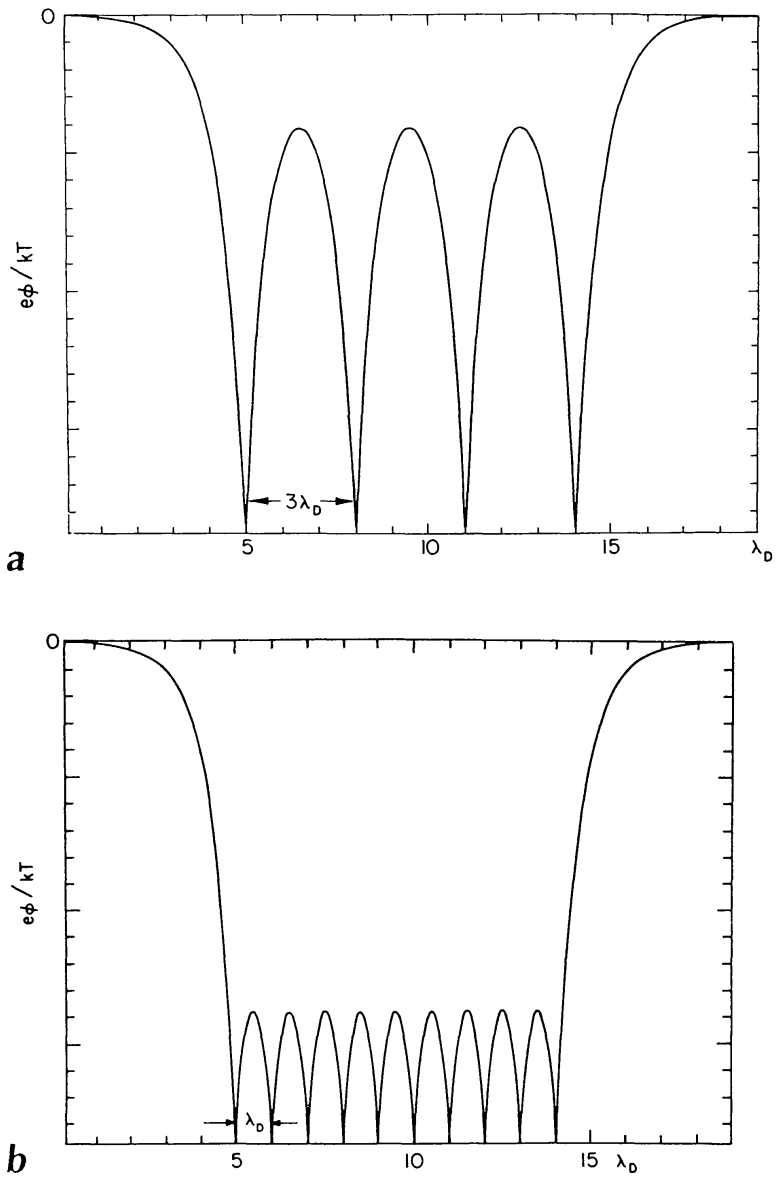

Figure 4 Steady state solution of the one-dimensional Poisson equation for grain sheets placed at regular intervals. The distance between grains is (*a*) $3\lambda_D$ and (*b*) λ_D. (From Goertz 1989.)

their analyses (Havnes et al 1984, 1987) to include a distribution of dust grain sizes and a photoemission charging current. A more detailed model developed by Wilson (1988) in connection with Saturn's rings includes many aspects of the rings' vertical structure as well as the proper solar illumination geometry. Besides photoelectron production, plasma absorption is also included. He finds that the electric field is more complicated in structure and stronger in magnitude within the cloud than at the edges.

The reduction of the magnitude of the grain charge when the intergrain spacing is reduced has recently been demonstrated experimentally. Xu et al

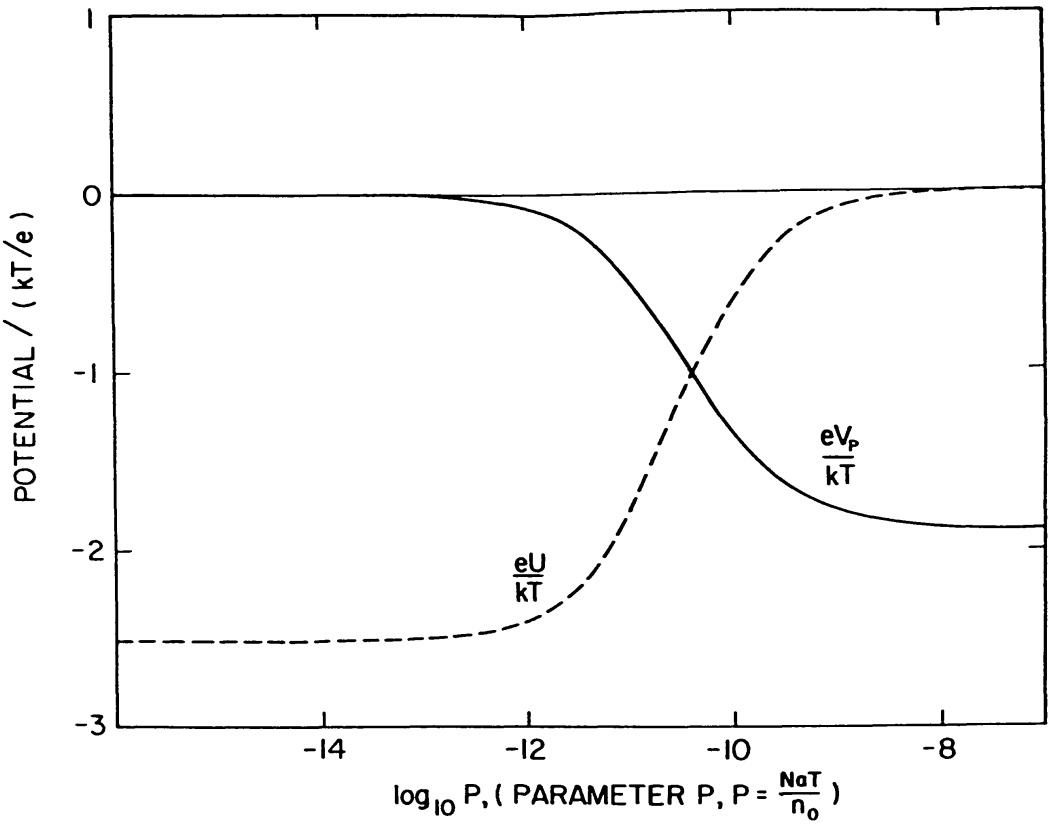

Figure 5 The variation of plasma potential V_p and grain potential U (proportional to the grain charge) as a function of P, i.e. dust density. T is the plasma temperature in electron volts, a is the grain radius in meters, and N and n_p are the dust and plasma densities, respectively. (From Goertz 1989.)

(1993) reported measurements showing how the average (negative) charge on a grain varies as the ratio of the intergrain spacing to the plasma Debye length is varied. For fixed dust density the dust charge density was found to decrease as the electron density decreases, i.e. as λ_D becomes $\gtrsim d$.

3. COAGULATION, DISRUPTION, AND LEVITATION OF CHARGED DUST

We now consider several of the physical effects manifested by charged dust.

3.1 *Coagulation*

The fact that the current-energy curve can have multiple roots in the presence of secondary emission led Meyer-Vernet (1982) to propose that grains with identical electrical properties, immersed in the same plasma but having different charging histories, could achieve opposite potentials. This idea was further

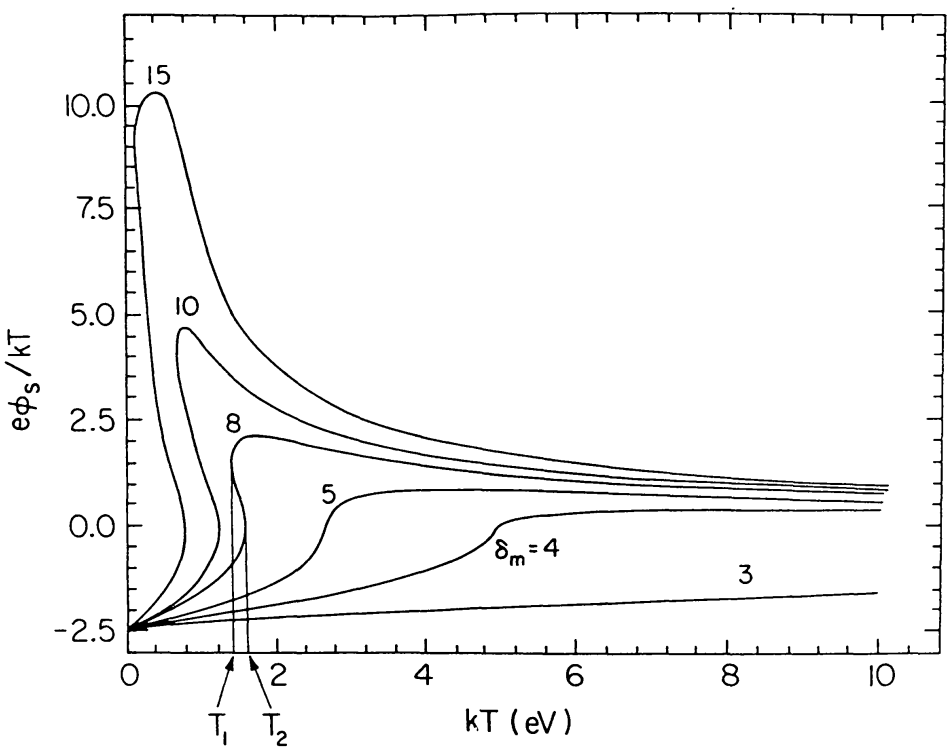

Figure 6 The equilibrium surface potential ϕ as a function of plasma temperature T for different values of the secondary yield parameters δ_m (the maximum yield). (From Goertz 1989.)

developed by Horanyi & Goertz (1990). The variation of the normalized grain surface potential $[\phi_s/(k_B T/e)]$ with plasma temperature (given in eV) for different values of δ_m is shown in Figure 6. Consider grains of different size immersed in the plasma and suppose that they all have the same δ_m (say 8). Now suppose that the temperature of the plasma is gradually increased. The potentials of all the grains will follow the $\delta_m = 8$ curve, but the large grains will respond faster. This follows from the fact that since $\frac{dQ}{dt} = I$, $\frac{a\phi_s}{\tau} \sim a^2$, and so the characteristic time τ required to reach the equilibrium potential corresponding to the instantaneous conditions $\sim 1/a$. Once the temperature increases beyond T_2 the grains clearly have to make a transition to the upper part of the curve, thereby changing the potential from a negative value to a positive value. Since the larger grains will collect the necessary positive charge to make this jump faster than the smaller grains, there will be oppositely charged grains in the plasma for some period of time. These authors studied the implication of this effect for grain coagulation; the attractive Coulomb force between the positively charged larger grains and the negatively charged smaller grains will naturally enhance the coagulation rate. Of course such coagulation can occur only during transient heating events, when the ambient plasma is temporarily heated, or when the grains move through a spatially confined hot plasma region.

Since the authors do not discuss the frequency and duration of such transient heating events in space, the efficiency of this process for grain coagulation remains uncertain.

Very recent work by Chow et al (1993) on secondary electron emission from small grains has shown that the dust grains of different sizes can acquire opposite charges in warm plasmas even in the absence of changes in the plasma environment. This is because the so-called Sternglass formula for the secondary emission yield $\delta(E)$, which is extensively used [including in the work of Meyer-Vernet (1982) and Horanyi & Goertz (1990)], applies only to the case of a semi-infinite planar slab, wherein the secondaries can escape only from one surface of the target, namely the side from which the primary electrons enter. For small grains (assumed spherical), secondary electrons are not limited to the point of entry of the primary electron; they can exit from all points on the grain surface. This increases the yield over that determined by using the Sternglass formula; the increase is very large for VSGs where the penetration depth of the primary electrons is comparable to its size, for a range of electron energies of interest (see Figure 7). There, the secondary electron yield obtained using the Sternglass formula would be very close to the curve marked "Jonker's" since the semi-empirical Sternglass formula (Sternglass 1954) approximates the theoretical derivation of Jonker (1952) for semi-infinite planar slabs. As expected the larger grains (diameter $D \gtrsim 1$ μm) follow the Jonker's yield curve. Chow et al (1993) have also calculated the equilibrium potential for conducting and insulating grains immersed in both Maxwellian and generalized Lorentzian plasmas. Due to this size effect on secondary emission they find that insulating grains with diameters 0.01 μm and 1 μm have opposite polarity (the smaller one being positive) when the plasma temperature is in the range 25–48 eV in a Maxwellian plasma. For Lorentzian plasmas this temperature range is shifted downward to 8–17 eV when $\kappa = 2$. These values may be in the range of the inferred values of $k_B T_e$ in many regions of the planetary ring systems (e.g. Goertz 1989) and comets (Mendis & Horanyi 1991) as well as in the interplanetary medium (Allen 1983), the local interstellar medium (Cox & Reynolds 1987), and supernova remnants (Raymond 1984). Furthermore, in the primordial protoplanetary nebula, if the kinetic energy of the gravitationally infalling gas was a source of ionization via the so-called critical ionization process (e.g. Alfven 1980) then electron thermal energies $\gtrsim 10$ eV may be possible at least in localized regions. Consequently, the existence of different sized grains of opposite polarity—negatively charged large grains and positively charged small grains—is possible in all of these environments. Enhanced coagulation à la Horanyi & Goertz (1990) would now take place, the only difference being that the larger grains will be always negative and the smaller ones always positive. Also, since transient heating effects are no longer necessary, the coagulation process should proceed continuously, and therefore more efficiently.

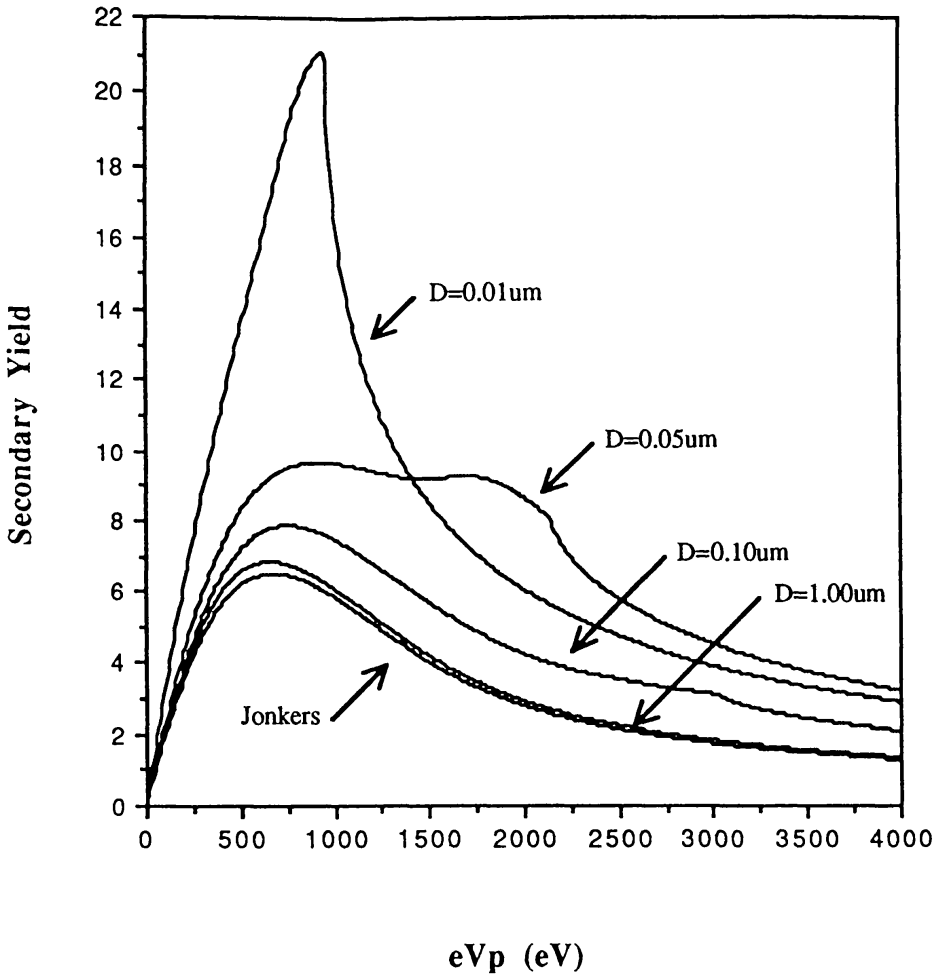

Figure 7 Secondary emission yield $\delta(E)$ as a function of the primary electron energy (eV_p) for different sized insulating grains (D). (From Chow et al 1993.)

In this connection it needs to be noted that photoemission too could cause grains to acquire opposite charges in the same plasma and radiative environment, even if they had the same size, provided they had widely different photoemission yields (Feuerbacher et al 1973). This also could lead to enhanced dust coagulation in certain regions of interstellar space as pointed out by the above authors.

3.2 *Disruption*

Coagulation is not the only physical effect of grain charging. Exactly the opposite effect, namely physical disruption of the grains could also occur if the grains acquire numerically very high potentials. This is a consequence of the electrostatic repulsion of like surface charges which produces an electrostatic tension in the body. If this electrostatic tension exceeds the tensile strength

of the body across any section, the body will break up across that section. Considering a sphere of uniform tensile strength, F_t, integrating the component of the Maxwell stress ($E^2/8\pi$) normal to the plane section of one hemisphere over its surface, and comparing it with the tensile force on that section, Opik (1956) showed that electrostatic distribution will occur across that section unless

$$F_t > F_e \left(= \frac{\phi^2}{8\pi a^2}\right), \tag{15}$$

where F_e is the electrostatic tension and a is the grain radius (all units are e.s.u. and c.g.s). For stability, this implies that

$$a > a_c (= 6.65|\phi| F_t^{-1/2}) \tag{16}$$

(where a_c is now measured in μm and ϕ is in volts, while F_t is in dynes/cm^2). It is clear from (15) that as a becomes smaller, the value of F_t required to prevent grain disruption increases rapidly. This also implies that as a grain begins to disrupt electrostatically it will continue to do so until reaching the smallest fragments for which the above macroscopic considerations apply (perhaps VSGs or clusters with $a \gtrsim 10$ Å). If this were so, it could also provide an insurmountable obstacle for grain growth in a plasma. What enables grains to circumvent this runaway disruption is the electric field emission of electrons from small grains, as was shown recently (Mendis 1991). This is because as the grain radius decreases, the surface electric field increases to such a value (typically $\gtrsim 10^7$ Vcm^{-1}) that rapid electron emission occurs from negatively charged grains and the grain potential decreases (numerically) to a value that is no longer given by the plasma environment but rather by the size alone, e.g. $|\phi| \approx 900a$ (Mendis & Axford 1974), where ϕ is in volts and a is in μm. Substituting the above value into Equation (15) we obtain the result that if $F_t > F_0 (= 3.6 \times 10^7$ dynes cm^{-2}), then the electric field emission limitation of the grain potential will prevent the electrostatic disruption of grains, regardless of their size. Consequently, materials such as iron ($F_t \sim 2 \times 10^{10}$ dyne cm^{-2}) and tektites ($F_t \sim 7 \times 10^{10}$ dyne cm^{-2}) are stabilized by this process against electrostatic disruption no matter how small the size. On the other hand, very fragile grains such as "cometary" grains $F_t (\approx 10^6$ dynes cm^{-2}) of very small radii (≈ 10 Å) will be stable only if $|\phi| \lesssim 0.15$ V, which corresponds to $T \lesssim 460$ K for a Maxwellian oxygen plasma and $T \lesssim 230$ K for a Lorentzian oxygen plasma with $\kappa = 2$.

It needs to be emphasized that the electric field emission effect will enable grain growth to take place in the above environments only if the grains are negatively charged. This means that if there is sufficient uv radiation to make the grain charge positive due to photoemission, grain growth will not proceed even in low temperature plasmas.

Fechtig et al (1979) suggested that the 2–3 orders of magnitude increase in the micrometeoroid flux (10^{-15}g $\lesssim m_d \lesssim 10^{-12}$g) observed within 10 $R_\oplus$ in the

terrestrial auroral regions by the *HEOS-2* satellite was due to such electrostatic disruption of type III "fireballs" of mass $\gtrsim 10$ g. This was shown to be unlikely since the tensile strength of these relatively large bodies would have to be improbably small for such a disruption to take place (Mendis 1981). On the other hand, since these bodies are expected to be highly irregular in shape, and since the electrostatic tension at any point in such a body is inversely proportional to the local radius of curvature, sharp edges and projections would get electrostatically chipped away as the body gets charged up (Hill & Mendis 1980a). Such a process of electrostatic "chipping" or erosion, rather than overall electrostatic disruption, has been proposed as the mechanism responsible for the aforementioned observation (Mendis 1981).

There are numerous examples of dust phenomena at comets that have been attributed to electrostatic disruption (see Mendis & Horanyi 1991 for a detailed review). These include the so-called pseudosynchronic bands or *striae* observed in cometary dust tails (Sekanina & Farrell 1980, Hill & Mendis 1980b); the discrete dust "packets" observed in the environment of comet P/Halley by the dust analyzers on the *VEGA* spacecrafts (Simpson et al 1987, 1989), and the peculiar spatial distribution of the VSGs ($10^{-20}\text{g} \lesssim m_\text{d} \lesssim 10^{-17}\text{g}$) also observed by the *VEGA 1* spacecraft at comet Halley (Sagdeev et al 1989, Fomenkova & Mendis 1992).

3.3 *Levitation*

Electrostatic charging can also lead to the levitation of fine dust lying on large surfaces. In this case, the charge Q acquired by the grain is proportional to its projected surface area (Singer & Walker 1962) and so $Q = \pi a^2 \sigma = \pi a^2 (E_n/4\pi) = a^2(\phi_\text{s}/4\lambda_\text{D}) = \left(\frac{a}{4\lambda_\text{D}}\right)(a\phi_\text{s})$. Typically $a/\lambda_\text{D} \ll 1$, and so the charge on the grain is very much smaller than that it would acquire in free space. Mendis et al (1981) considered the charging of the bare cometary nucleus by the solar wind plasma and solar uv radiation at large heliocentric distances. They showed that while the subsolar point of the cometary surface acquires a positive potential of $\sim +5$ V due to the dominance of photoemission, the nightside could acquire a negative potential $\approx -m_\text{p} V_\text{sw}^2/2e$, (which ~ -1 kV when $V_\text{sw} \approx 600$ km/sec). Consequently, submicron-sized grains could overcome the gravitational attraction of the nucleus and levitate on the nightside of the comet, even when they had a deficit of just one electron charge. Since the nightside potential is highly modulated by the solar wind speed ($\sim V_\text{sw}^2$), grains are more likely to be electrostatically levitated and subsequently blown off the dark surface when the comet intercepts a high-speed solar wind stream. The sporadic brightness variations of comet Halley observed inbound at large heliocentric distances ($\sim$11–8 AU) were attributed to this effect by Flammer et al (1986). These authors showed that the comet encountered a corotating high-speed solar wind stream emanating from a southern coronal hole at the times of

the observed brightness increases. More recently, a large brightness increase of comet Halley at a heliocentric distance ≈14.3 AU (outbound) has also been attributed to a solar flare–generated shock wave moving at a speed ~750 km/sec at that distance (Intrilligator & Dryer 1991). These authors suggest that the dust results from the pressure-induced rupture of the nucleus. This is very unlikely because the ram pressure at 14.3 AU, which is estimated $\sim 3 \times 10^{-9}$ dynes/cm^2, is far too small for the purpose. It is much more likely that the physical process responsible for the dust emission is electrostatic levitation from the nightside of the comet, as discussed earlier.

4. DYNAMICS

About 20 years ago Mendis & Axford (1974) discussed the basic nature of the trajectories of interplanetary dust grains entering planetary magnetospheres, getting charged to significant negative potentials within the plasmaspheres, and moving under the combined influence of planetary gravity and the Lorentz force. Since then there has been a growing body of literature on the dynamics of charged dust in planetary magnetospheres and the cometary environment.

The basic equation governing the dynamics of a charged dust grain of mass m_d, velocity $\mathbf{v}_d$, in the planetocentric inertial frame is

$$m_d \frac{d\mathbf{v}}{dt} = Q(t)\left[\mathbf{E} + \frac{\mathbf{v}_d \times \mathbf{B}}{c}\right] - \frac{GM_p m_d}{r^3}\mathbf{r} + \mathbf{F}_d + \mathbf{F}_r + \mathbf{F}_c. \tag{17}$$

In the region of the magnetosphere that is corotating with the planet of mass M_p with angular velocity $\boldsymbol{\Omega}_p$, $\mathbf{E} = -(\boldsymbol{\Omega}_p \times \mathbf{r}) \times \mathbf{B}/c$, and $\mathbf{F}_c$, $\mathbf{F}_r$, and $\mathbf{F}_d$ are forces associated with collisions of the grain with plasma, radiation, and other grains respectively. The force $\mathbf{F}_c$, which arises from the relative motion between the grain and the plasma, has contributions both from the direct impacts with ions as well as from Coulomb interactions between the grain charge and the ions, and has been discussed at length by Northrop & Birmingham (1990). However, it was shown to be of negligible importance to the dynamics of charged dust in the magnetospheres of Jupiter and Saturn (e.g. Hill & Mendis 1980b, Mendis et al 1984), and plays only a marginal role in orbital evolution (e.g. Northrop et al 1989). The force $\mathbf{F}_r$ due to radiation pressure is also negligible in the Jovian and Saturnian magnetospheres, but is of crucial importance in the terrestrial magnetosphere, due to its greater proximity to the Sun (e.g. Horanyi & Mendis 1986a). Finally, $\mathbf{F}_d$ is negligible in all cases. The Lorentz force, due to the relative motion between the charged dust and the planetary magnetic field, however, can be comparable to the gravitational force for submicron-sized grains charged to reasonable potentials (e.g. see Mendis et al 1982).

Mendis et al (1982) discussed the epicyclic motion of charged dust in the equatorial plane of a planet whose magnetic and spin axes are parallel or

antiparallel. In this case the corotational electric force is always radial. In the case in which Q/m_d is sufficiently large numerically that this motion may be described by the guiding-center approximation, and the net radial force is attractive, the guiding center will perform a circular orbit around the planet with an angular velocity Ω_G given by

$$\Omega_G^2 + \omega_0\Omega_G - \omega_0\Omega_p - \Omega_K^2 = 0, \tag{18}$$

where $\omega_0 = -QB/m_dc$ and $\Omega_K[= (GM_p/r^3)^{1/2}]$ is the Kepler angular velocity. The grains themselves will gyrate around the magnetic field lines with an angular velocity ω in an elliptical orbit whose minor axis is always radial, and whose axis ratio, b/a, is given by

$$\frac{b}{a} = \frac{-\omega}{\omega_0 + 2\Omega_G} \tag{19}$$

with

$$\omega^2 = \omega_0^2 + 4\omega_0\Omega_G + \Omega_G^2. \tag{20}$$

In the case of Saturn, where the magnetic and spin axes are known to be parallel (at least to within 0.5°), if the grains are negatively charged the ellipse is performed in the retrograde sense while the guiding center motion is direct. It is easily seen from Equations (18), (19), and (20) that when $-Q/m_d \to \infty, \Omega_G \to \Omega_p, \omega \to \omega_0$, and $b/a \to 1$, and we recover the purely electrodynamic case. When $Q/m_d \to 0, \Omega_G \to \Omega_K, \omega \to +\Omega_K$, and $b/a \to 1/2$, and we recover Keplerian motion. In the general gravito-electrodynamic case: $1/2 < b/a < 1$ and $\Omega_K < \Omega_G < \Omega_p$ outside the synchronous radius (i.e. where $\Omega_K = \Omega_p$) and $\Omega_p < \Omega_G < \Omega_K$, inside.

As a consequence of the fact that $\Omega_G > \Omega_K$ outside the synchronous orbit Mendis et al (1982) pointed out that grains of a particular size in the F Ring could be in resonance with the inner "shepherding" satellite S27 of this ring. They consequently argued that the peculiar "wavy" nature of this ring, which is known to be composed largely of micron and submicron-sized dust, could be caused by such a novel "magneto-gravitational" resonance. However, it was subsequently shown (e.g. Grun et al 1984) that the charge on individual grains in the F Ring (where $\lambda_D \gtrsim$ the average integration distance) has a much smaller value than the "isolated" grain value assumed by Mendis et al (1982) and as a result could not lead to waves of the observed wavelength. In the analysis of Mendis et al (1982), the grain charge was assumed to be constant. However, more general treatment of the adiabatic motion of charged grains in planetary magnetospheres, which also takes into account the periodic variation of the grain charge, was given by Northrop & Hill (1983a). There are several causes for the periodic variation of the grain charge. One results from the variation of the total velocity of the grain at the gyrofrequency due to the gyration of the

grain about the guiding center. This in turn causes a variation of the ion current (as discussed earlier) and thus of the grain potential with the same frequency. Others result from temperature gradients that may be present in the plasma as well as compositional variations, since both these result in periodic variations of the plasma collection currents at the gyrofrequency. Since all guiding center drifts may be regarded as being due to the variation of the gyroradius at the gyrofrequency, these could give rise to additional drifts of the guiding center. These drifts would also be azimuthal if the maximum and minimum grain potentials were achieved at the largest and smallest radial distances from the planet. This, however, is not the case, due to the small but finite electrical capacitance of the grain, which leads to a phase lag in the grain potential with respect to the radial oscillation. Thus the maximum and minimum potentials are reached at a small angular distance from the positions of maximum and minimum distances from the planet giving rise to a radial component in the drift. This drift has been dubbed the "gyrophase drift" by Northrop & Hill. Incidently, density gradients in the plasma periodically change the response time for charging and therefore the aforementioned phase lag. This in turn, changes the radial gyrophase drift rate. The direction of the drift depends not only of the polarity of the grain charge and on whether it is inside or outside the synchronous radius, but it also depends on the directions of the temperature and compositional gradients and on the ratio of the grain velocity with respect to the ion thermal velocity (see Figure 2). The variation of the grain charge at the gyrofrequency destroys the adiabatic invariance of the magnetic moment. However, the analysis of Northrop & Hill (1983a) led to the identification of another exact constant of the motion, which enabled them to find the so-called circulation radius where the magnetic moment became zero and stopped the radial drift. In the earlier numerical calculations of Hill & Mendis (1980b) of negatively charged grains in an assumed isothermal Jovian magnetosphere, the interplanetary grains that entered the magnetosphere and got charged did drift towards the synchronous radius, at the progressively slowing rate due to the decrease of the magnetic moment and consequent circularization of the orbits. However, what Northrop & Hill (1983a) showed was that circularization of the orbits and consequent cessation of the gyrophase drift depended on the geometry of the initial launch and could therefore take place before the synchronous radius was reached.

From a reexamination of one of the last *Voyager 2* photographs of Jupiter in forward-scattered light, as the spacecraft left the planet, Showalter et al (1985) discovered a very tenuous ring, composed largely of fine micron and submicron-sized dust, and extending outward from the brighter thin inner ring ($\sim 1.82 R_J$) to the vicinity of the satellite Thebe ($\sim 3.11 R_J$). The most interesting feature of this, so-called gossamer ring (see Figure 8) is the significant peak exactly at the synchronous radius (2.24 R_J). Showalter et al (1985) believed that the sources

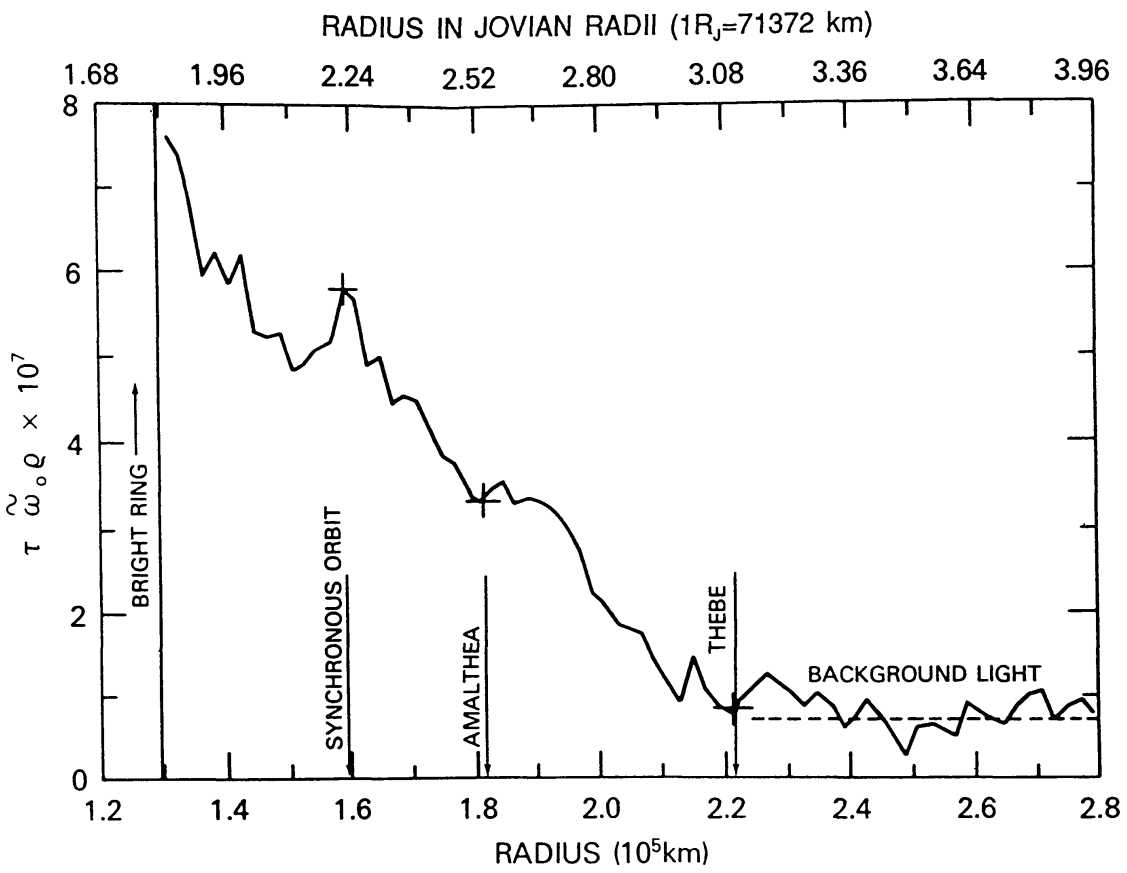

Figure 8 The gossamer ring. The ordinate is proportional to the intensity of scattered light. (Reproduced from Showalter et al 1985.)

of these rings were larger bodies ("mooms") straddling the synchronous orbit, and that the dust emitted from these mooms drifted away from the synchronous orbit in both directions due to plasma drag. A subsequent detailed analysis by Northrop et al (1989) showed that the gyrophase drift of small grains could greatly exceed the drift due to both the plasma drag and the Poynting-Robertson (radiation) "drag." While this gyrophase drift can cause the dust to drift both towards or away from the synchronous orbit, a maximum plasma temperature near the synchronous orbit could cause the grains to concentrate there since temperature-associated gyrophase drift is always towards the higher temperature. These authors suggest that the satellite Amalthea, rather than unobserved mooms, is the source of this dust. They also show that the satellite Io ($\sim 6R_J$), which is known to be a source of dust due to volcanic activity, is unlikely to be the source of at least the smaller dust particles in the gossamer ring, due to a very large plasma temperature gradient at the inner edge of the Io plasma torus. However, they concede that larger grains may penetrate this barrier due to a radial diffusion caused by the stochasticity of the number of charges residing on the grain at a given time, as proposed earlier by Morfill et al (1980).

One of the most intriguing features observed in the Saturnian ring system by both *Voyagers 1* and *2* was the near-radial spokes (Smith et al 1982), which more than anything else, provided the impetus for the study of dust-plasma interactions in planetary magnetospheres. These spokes are confined to the dense central B Ring with inner edge at 1.52 R_s and outer edge at 1.95 R_s. They have an inner boundary at $\sim$1.72 R_s and an outer boundary at approximately the outer edge of the B Ring. Against the background of the B Ring they appear dark in backscattered light and bright in forward-scattered light, indicating that they are composed of micron and submicron-sized grains.

A typical spoke pattern is seen in Figure 9. The spokes exhibit a characteristic wedge shape (clearly apparent in the central spoke of the Figure); the vertex coincides with the position of the synchronous orbit at $\sim$1.86 R_s. Movies of

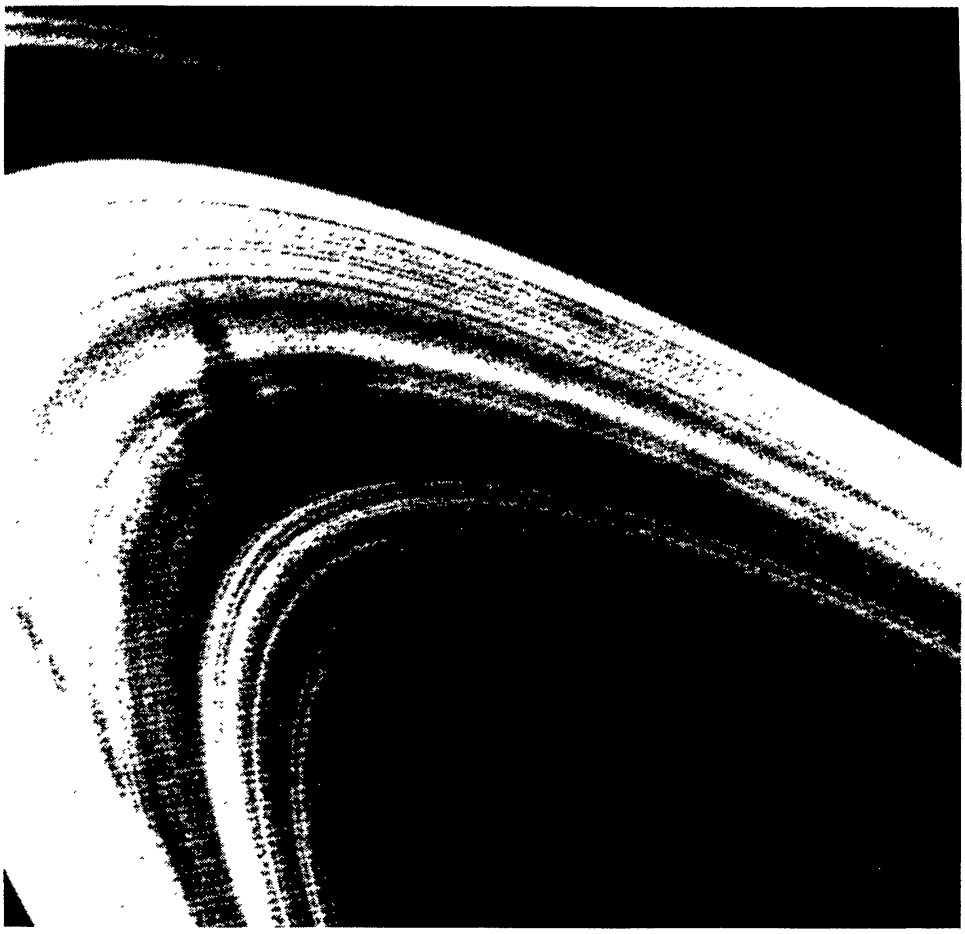

Figure 9 Image of spokes in the B Ring. Note the distinct wedge shape of the spoke at the upper left portion of the picture. The vertex of the wedge is near the synchronous orbit. The rotation is counter clockwise with the leading edge being the slanted one. (*Voyager 2* photograph from Smith et al 1985.)

the observational data show the formation and dynamical evolution of these spokes. They are more easily seen and seem to be more sharply defined on the morning ansa as they are rotated out of Saturn's shadow. High-resolution *Voyager 2* images show that the leading and trailing edges of the spokes have distinctly different angular velocities. Inside the synchronous orbit where these spokes are seen most often, the leading tilted edge has essentially the Kepler value, whereas the trailing near-radial edge has approximately the corotational value. Based on the observing geometry, it has been argued that the material constituting the spokes is elevated above the ring plane (Smith et al 1982, Grun et al 1983). Several theories were quickly proposed to explain the formation and evolution of these spokes. While all of them involved electrical effects to produce the spokes, many of them specifically involved electrostatic levitation. [For a detailed review of these theories, see e.g. Mendis et al (1984).] The most detailed of these theories was the one due to Goertz & Morfill (1983). Since the intergrain distance in the B Ring is less than the Debye length, they treat the entire ring as a uniformly charged disc and assuming that the electron density near this disc is provided largely by photoelectrons they estimate that the ring potential is $\sim +5$ V. Under these circumstances only a small fraction of micron-sized grains will have even one electronic charge, as discussed in Section 3. Consequently, the grains are unlikely to be electrostatically levitated against the gravitational attraction of the ring. A much denser source of plasma is required to make the levitation process feasible.

Noting that spoke formation is a sporadic process, Goertz & Morfill (1983) proposed that such dense localized plasma columns are produced by meteor impacts with the ring particles. Initially, a very dense ($n_e \approx 10^{15}\text{cm}^{-3}$) plasma cloud is formed, which expands rapidly while diamagnetically excluding the magnetic field until the diamagnetic factor $\beta \approx 1$. The neutral gas cloud produced by meteor impact will be photoionized. Losses through the loss cone to Saturn's atmosphere and via ring absorption will continue. The plasma column will initially move with the speed of the meteor target until $n_e \leq 10^2\ \text{cm}^{-3}$, whereafter it will tend to corotate. During such conditions not only can small fine dust (typically $R_g \approx 0.1\ \mu$m) be electrostatically levitated off the ring plane, but the plasma column itself will move radially. This is due to the fact that the relative motion between the charged dust (which is close to Keplerian) and the surrounding plasma (which is corotating) constitutes a current. Since this current is confined azimuthally to the plasma column, it must close through the ionosphere via a Pedersen current which is connected to the dust-ring current by a pair of field-aligned currents (Figure 10). The Pedersen current sets up an electric field in the ionosphere, which then maps back onto the ring plane and causes a radial $\mathbf{E} \times \mathbf{B}$ drift of the plasma cloud. Knowledge of the ionospheric Pedersen conductivity ($\Sigma_p \approx 0.1$ mho) leads to the calculation of the radial velocity V_R of the plasma column which ranges from $\approx$45 km s^{-1}

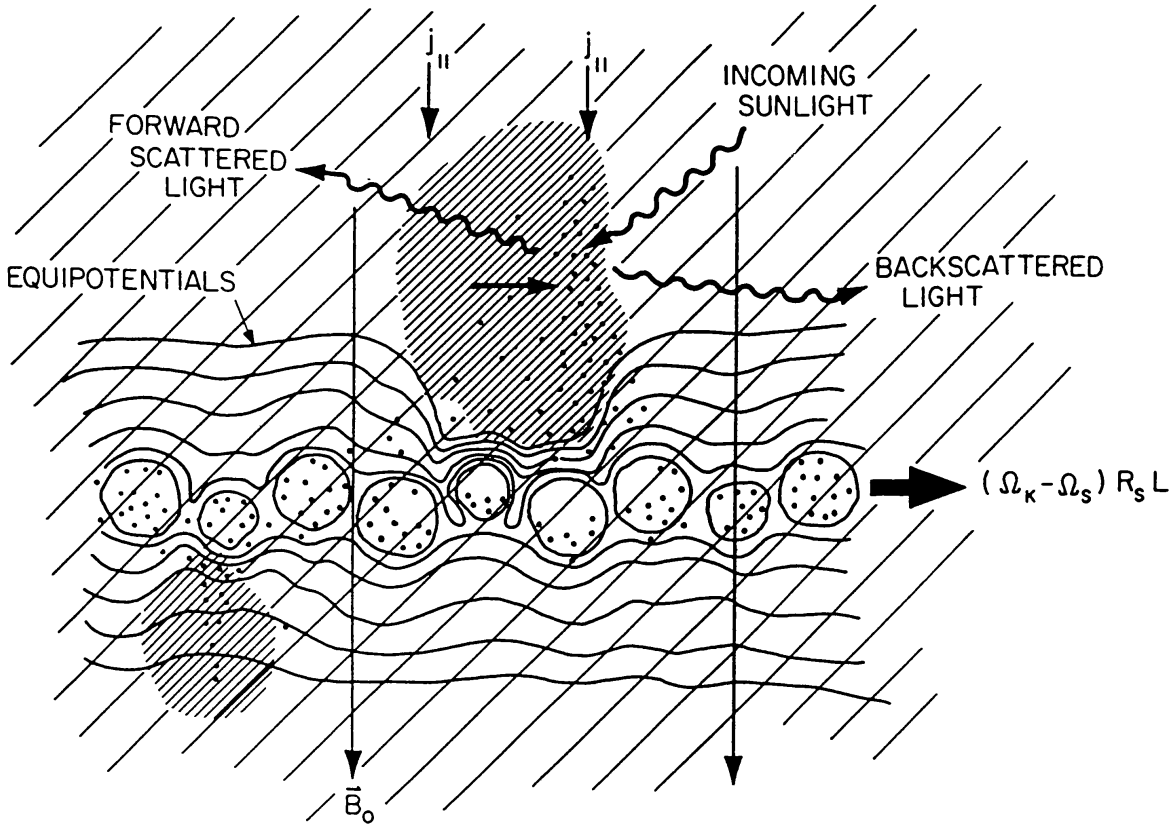

Figure 10 A schematic view of the model for formation of spokes. Underneath a dense plasma column (indicated by heavy shading) the equipotential contours are compressed and a large surface electric field exists. Dust particles are lifted off the rings and drift through the cloud which polarizes. A pair of field-aligned currents closes the current. (Figure from Goertz & Morfill 1983.)

at $L = 1.7$ (the inner edge of the spoke region) to zero at the synchronous orbit ($L = 1.86$). At $L = 1.9$, the outer edge of the B Ring, $V_R \approx 23$ km s^{-1}. As such a plasma column moves from its position of creation, it will leave behind a radial trail of dust much like a car racing across a dusty plain. Goertz & Morfill suggested that the observed spokes are formed in this way.

An alternative mechanism for spoke formation was proposed earlier by Hill & Mendis (1982a). While they too propose that small grains constituting the spokes are electrostatically levitated and blown off the surfaces of larger bodies when they are charged to high electrostatic potentials, they suggest that the sporadic field-aligned beaming of energetic electrons accelerated at electrostatic double layers high up in Saturn's ionosphere may produce the high surface potentials necessary for this process. They suppose that these double layers are highly confined in longitude but extended in latitude, so as to account for the radial extent of the thin spokes. While double layers are known to occur in the Earth's magnetosphere, they do so on field lines connected to the auroral region, where field-aligned currents flow from the magnetotail. The field lines

threading the B Ring of Saturn are closed ones, and the question arises as to how such double layers could be generated there, because the flow of field-aligned currents constitutes a necessary condition for their formation on the field lines. The answer perhaps lies in the fact that the relative motion between the ring dust and the plasma constituted a novel type of dust ring current (Hill & Mendis 1982b). Ip & Mendis (1983) showed that this dust ring current is diurnally modulated by Saturn's shadow. Continuity of this current leads to field aligned currents that close through the ionosphere. This could lead to the formation of double layers high up in the ionosphere which will accelerate electrons down into the equatorial plane in the morning ansa, close to the terminator. This is consistent with observations of high spoke activity in this region.

While on the subject of the dust ring current, we note that Houpis & Mendis (1983) have attributed the observed fine ringlet structure of the ring to the resistive tearing of this dust ring current.

A very interesting and far-reaching consequence of the spoke formation due to meteorite bombardment was subsequently deduced by Shan & Goertz (1991), by asking the question as to what happens to the levitated dust. The component normal to the ring plane gives a charged dust particle a gravitoelectrodynamic trajectory which causes it to reintersect the ring plane about 180 degrees away in azimuth from its point of levitation and at different radial distance from the planet. If it collides with a ring particle at that point it will transfer angular momentum to it because its specific angular momentum is different from that of its target. This will cause the target body to move either inward or outward depending on whether its own specific angular momentum is larger or smaller than that of the projectile. Starting with an initial uniform distribution of mass in the region of the B Ring and assuming that the micrometeoroid bombardment rate remains constant at the present-day level, Shan & Goertz (1991) studied the redistribution of mass due to the above process. They found that the calculated profile closely matched the observed profile seen in Figure 11 after a period of $(4–8) \times 10^8$ yrs. If this mechanism is indeed responsible for the observed B Ring profile, and if one accepts the assumption of the constant rate of meteorite bombardment, one is led to the important conclusion that the observed ring system is significantly younger than the Solar System (age $\sim 4.5 \times 10^9$ yrs). Entirely different lines of argument (Borderies et al 1984, Connerney & Waite 1984, Northrop & Connerney 1986) lead to even smaller ages for the ring system ($\sim 4 \times 10^6$–7×10^7 yrs). These age estimates seem to contradict an earlier view that this ring system is a relic left from the formation of the Saturnian system $\sim 4.5 \times 10^9$ yrs ago (Alfven 1954). If indeed the rings were formed after the formation of Saturn the most likely scenario is the disruption of a moon ($\sim 3 \times 10^{22}$ g) by a large comet ($\sim 10^{18}$ g). However, Lissauer et al (1988) have concluded, from the cratering history of Saturn's present moons, that it is very unlikely that the rings were formed by such a disruption of a moon

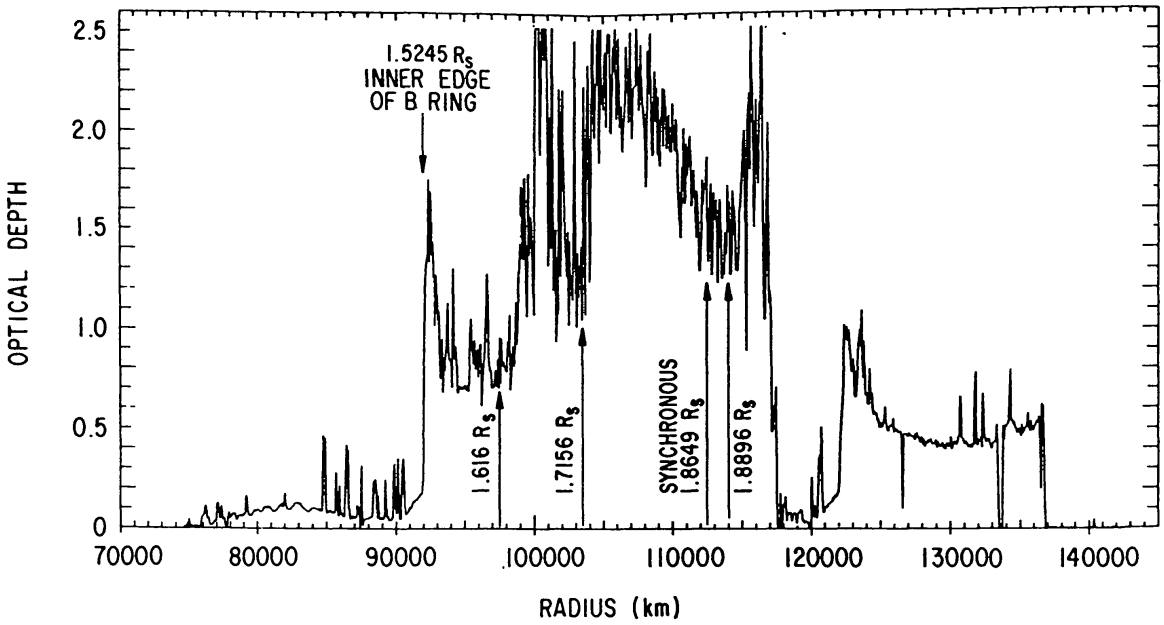

Figure 11 Optical thickness of the A, B, and C rings of Saturn. (A ring 122,000–137,000 km, B ring 92,000–118,000 km, and C ring 75,000–92,000 km.) (From Northrop & Hill 1983b.)

within the last 10^9 yrs. So the question of the age of the ring system remains unresolved.

Several studies based on dust-plasma interactions have also been used to explain the sharp discontinuities observed at $\sim 1.62 R_s$, and at the inner edge of the B-Ring at $\sim 1.524 R_s$ (Northrop & Hill 1982, 1983b; Ip 1983). These have been extensively reviewed elsewhere (e.g. Mendis et al 1984) and are not further discussed here, except to mention that all these involve the upward siphoning of dust impact-produced plasma or very small charged grains, with large numerical values of Q/m_d inside some critical radius within a corotating magnetosphere.

Horanyi et al (1990; see also Horanyi et al 1991) studied the dynamics of submicron-sized dielectric grains ejected from the small Martian satellite Phobos due to micrometeoroid bombardment. They found that these grains were influenced not only by gravity but also by solar radiation pressure and Lorentz forces. They concluded that any grains that remain in the vicinity of the orbit of Phobos are the ones that are governed mainly by gravity and are thus much larger than 1 μm. Very small ($a < 0.2$ μm) grains are removed from the Martian-environment very rapidly, whereas larger submicron-sized grains remain in orbit around Mars for several months forming a nonuniform, time-dependent dust halo.

Horanyi & Burns (1991) studied the effect of planetary shadows on the dynamics of charged dust grains in motion around the planets. Since the photoelectron current is periodically shut off in the shadow, the charge in the grain potential and thus the electromagnetic perturbation resonates with the orbital

period, and can rapidly change the size and eccentricity of the grain orbits. In an earlier study, Hill & Mendis (1982c) came to a similar conclusion. They attributed the unusually large eccentricities of isolated ringlets, located in relatively transparent regions of Saturn's ring system, where presumably the plasma density is relatively high, to such a shadow resonance. They also argued that very small grains of certain sizes could be rapidly removed from these regions, due to so-called gyro-orbital resonances, i.e. when $\Omega_G/\omega = 2,\ 3$, etc (see Equations 18 and 20).

When the magnetic field of a planet is not an aligned and centered dipole, a charged dust particle orbiting the planet will experience a time-variable Lorentz force even if the orbit is circular and in the equatorial plane and the grain charge is constant. If the orbital frequency of the dust particle is commensurate with the frequency of this variable Lorentz force it can undergo large out-of-plane and radial excursions as shown by Burns et al (1985) for charged Jovian ring particles. In particular, they show that the outer edge of the lenticular Jovian dust halo (see also Consolmagno 1983) coincides with a low-order resonance of the above type.

Recently Horanyi et al (1992) have studied the motion of charged dust launched from the Saturnian satellite Enceladus ($\sim 3.95 R_s$). In this study they take into account the oblateness of Saturn's gravity field as well as the obliquity of Saturn's orbit around the Sun. While giving rise to novel effects, the calculated dust distribution has many of the observed characteristics of Saturn's E-Ring ($3R_s \lesssim r \lesssim 8R_s$).

One of the most unexpected observations of the recent *Ulysses* mission to Jupiter was the detection of quasi-periodic ($\sim$28 days) high-speed (20–56 km/sec) streams of submicron-sized grains (1.6×10^{-16} g $< m_d < 1.1 \times 10^{-14}$ g), during its distant Jovian encounter. Horanyi et al (1993) conclude that the initial source of these grains, which appear to come from the Jovian magnetosphere, are the observed volcanic eruptions on the Jovian satellite Io. They find that the Lorentz force on these charged grains of radius $\lesssim 0.1$ μm is sufficient to overcome Io's gravity and inject them into the Jovian magnetosphere. There the grains acquire a potential $\sim +3$ V (outside the Io plasma torus) due to the dominance of secondary emission, and while the smallest grains ($a \lesssim 0.02$ μm) remain tied to the magnetic field and tend to corotate with it, those in the size range $0.02 \lesssim a \lesssim 0.1$ μm get slung out from the magnetosphere (see Figure 12). These particles are in the correct mass range of the detected particles; their calculated velocities (30 km s$^{-1} \lesssim v \lesssim$ 100 km s^{-1}) also roughly correspond to the observed velocities. Horanyi et al also provide a plausible explanation to the observed periodicity of these streams on the basis of the dependence of the exit direction of the escaping grains on both the geographic and the geomagnetic coordinates of Io.

The dusty cometary environment is an ideal cosmic laboratory for the study

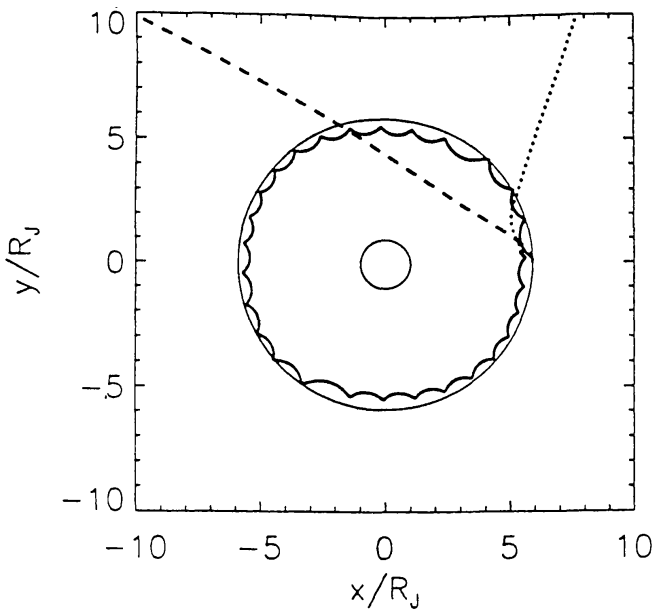

Figure 12 The trajectories of dust particles with size $a = 0.02$ (*solid curve*), 0.03 (*dotted line*) and 0.1 μm (*dashed line*) started from Io. At $t = 0$ the longitude of Io is zero in both the inertial frame and in magnetic coordinates. The two circles represent the surface of Jupiter and Io's orbit. (From Horanyi et al 1993.)

of the physical and dynamical consequences of dust-plasma interactions. Indeed, there exists a growing number of both remote and in-situ observations of cometary phenomena that attest to such interaction. Some of the physical consequences have already been discussed in Section 3. Among the dynamical consequences are (*a*) the asymmetry of sunward dust envelopes of certain comets (Wallis & Hassan 1983), (*b*) the overall spatial distribution of dust at comets P/Giacobini-Zinner and P/Halley (Horanyi & Mendis 1986a, b), and (*c*) the "wavy" appearance of the dust tail of comet Ikeya-Seki (1965f) (Horanyi & Mendis 1987).

The cometary dust particles, which are entrained by the gas sublimating from the nucleus, are immersed in a plasma and radiative environment, and are thus electrically charged. Outside the cometary ionopause (which separates the outflowing cometary ions from the inflowing, contaminated solar wind plasma), the plasma is magnetized. The equation governing the motion of a charged dust particle in the cometocentric inertial frame is given by an equation analogous to (17). The main difference from the planetary case is that the gravitational force of the small cometary nucleus is negligible, whereas the radiation pressure force $\mathbf{F}_r$, is not. $\mathbf{E}$ represents the convectional electric field $-\mathbf{v}\times\mathbf{B}/c$, where $\mathbf{v}$ is the velocity of the contaminated solar wind plasma relative to the cometary nucleus. As in the planetary case, $\mathbf{F}_c$ and $\mathbf{F}_d$ are negligible. In the dense cometary ionopause where $T_e \lesssim 10^3$ K and $n_e \gtrsim 10^3$ cm^{-3}, the

grain potential $\phi \sim -0.2$ V. In the region of largely undisturbed solar wind, where photoemission is dominant $\phi \sim 2$–5 V, whereas in the region between the outer cometary bow shock and the ionopause the grain potentials could have both positive and negative values. While conducting grains (e.g. C) may remain negative throughout ($\phi \sim -10$ to -20 V), dielectric grains (e.g. silicates) could switch from being negative closer to the ionopause to being positive closer to the bow shock due to the importance of secondary electron emission in the later region (e.g. Wallis & Hassan 1983). The electrostatic acceleration of the grain is given by $\mathbf{g}_e = -Q(\mathbf{v} \times \mathbf{B})/cm_d$, since $|\mathbf{v}_d| \ll |\mathbf{v}|$. The acceleration due to solar radiation pressure is given by $\mathbf{g}_r = (Q_{pr}/c) \cdot (L_0/4\pi r^2) \cdot (\pi a^2/m_d)$, where Q_{pr} is the scattering efficiency for radiation pressure and L_0 is the mean solar luminosity ($\approx 3.90 \times 10^{33}$ erg s^{-1}). To a good approximation $\mathbf{E}$ is constant outside the ionopause along the sun-comet axis. Assuming that $|\mathbf{B}| = 5\gamma$ and that $\mathbf{B}$ is inclined at 45° to V_{SW} at 1 AU, one obtains

$$X = \frac{|\mathbf{g}_e|}{|\mathbf{g}_r|} = \frac{10^{-2}|\phi|}{Q_{pr}a(\mu)}, \tag{24}$$

where ϕ is in volts.

The values of X for different sized grains are given in Table 2, where it is assumed that $|\phi(V)| = 5$. It is seen that $X \ll 1$ when $a = 1\mu$, but $X \approx 0.28$ for Magnetite and $X \sim 1$ for Olivine when $a \approx 0.1\mu$. When $a = 0.03\mu$, $X \gg 1$ for Olivine. As Wallis & Hassan (1983) pointed out this is the reason why the sunward dust envelopes (which are the envelopes of the trajectories of the grains emitted from the nucleus and which are moving under the acceleration $\mathbf{g}_e + \mathbf{g}_r$) are skewed away from the sun-comet axis. If $\mathbf{g}_g = \mathbf{0}$, clearly the apex of these envelopes will lie on the sun-comet axis.

Horanyi & Mendis (1986a,b) subsequently performed numerical simulations to calculate the distribution of charged dust grains in the environments of comments P/Giacobini-Zinner and P/Halley, using plasma and magnetic models of calculate $\phi(t)$. In these calculations, the orbital motion of the comet was also taken into account. In the case of comet P/Giacobini-Zinner, a scatter

Table 2 Ratio of X for different sized grains in the cometary environment[a]

$a(\mu m)$	X	
	Olivine	Magnetite
1.0	0.05	0.04
0.5	0.85	0.06
0.1	1.00	0.28
0.03	16.5	3.35

[a]From Mendis & Horanyi (1991).

plot of the distribution of the grains of various sizes in a plane normal to the sun-comet axis, at a distance of 10^4 km behind the nucleus, is shown in Figure 13. In this case, the interplanetary magnetic field is assumed to be in the orbital plane of the comet, so that the convectional electric field is normal to this plane.

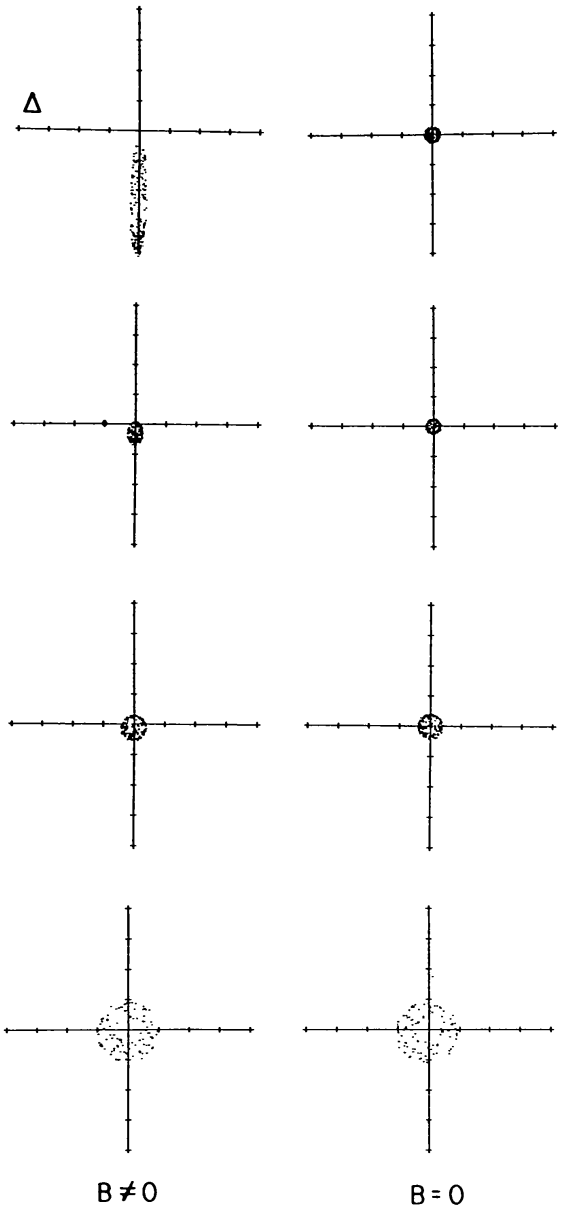

Figure 13 The distribution of dust grains of various sizes (top to bottom, 0.03 μm, 0.1 μm, 0.3 μm, and 1.0 μm) in a plane normal to the Sun-comet axis at a distance 10^4 km down the tail of comet P/Giacobini-Zinner. The left column shows the scatter plots of the dust distributions when the interplanetary magnetic field is included. The right column shows the corresponding scatter plots when the interplanetary magnetic field is excluded. (From Horanyi & Mendis 1986b.)

The grain sizes increase from 0.03 μ at the top of the Figure to 1.0 μm at the bottom. The first column shows the distributions when the electromagnetic effects are taken into account ($\mathbf{B} \neq \mathbf{0}$); the second column shows the corresponding distributions when the electromagnetic effects are neglected (e.g. $\mathbf{B} = \mathbf{0}$). The nucleus in each plot is located at the origin of coordinates. The elongation of the distribution normal to the orbital plane is obvious, particularly for the smallest grains (0.03 μm). In that case, it is also seen that the grains are concentrated well below the orbital plane. The larger grains have a more symmetrical distribution about the axis. In the absence of electromagnetic effects (e.g. $\mathbf{B} = \mathbf{0}$), it is seen, once more, that the larger ("older") grains concentrate away from the axis, while the smaller ("younger") grains concentrate closer to the axis. These distributions are, of course, axially symmetric in this case.

The NASA *ICE* spacecraft intercepted the tail of comet Giacobini-Zinner on September 11, 1985, at a distance of about 8×10^3 km from the nucleus, moving in a generally south to north direction in the comet's reference frame. Although the spacecraft did not carry a dust detector, the plasma wave instrument detected impulsive signals that were attributed to dust impacts on the spacecraft (Gurnett et al 1986). Although an asymmetry in the impact rate between the inbound and outbound legs consistent with the prediction for charged grains was indeed observed (see Figure 14), the asymmetry was rather small and may also be consistent with nonisotropic emission of grains from the nucleus, as suggested by Gurnett et al (1986). However, this observation coupled with the observation that the smaller particles were encountered farther away than the larger ones and also had a greater asymmetry between the two legs (Gurnett et al 1986) strongly supports the charged dust model. If the grains were not charged, the larger ones would have been encountered before the smaller ones.

Besides naturally occurring dust, there is now a significant component of anthropogenic dust in the terrestrial magnetosphere. Small (0.1–10 μm)Al_2O_3 spherules are dumped into the Earth's lower magnetosphere during solid rocket motor burns used for transfer of satellites from low earth to geosynchronous orbit. The flux from one such burn could exceed the natural micrometeoroid flux in that size range (Mueller & Kessler 1985). Although solar radiation pressure plays the dominant role in the orbital evolution of much of this dust, electromagnetic effects, as described for the more distant magnetospheres of Jupiter and Saturn, play a crucial role at the lower end of the dust mass spectrum ($a \lesssim 0.1$ μm). In that case, these electromagnetic forces conspire with solar radiation pressure to eliminate these grains from the magnetosphere in a comparatively short time, while significantly changing the residence time of large ($0.1\mu \lesssim a \lesssim 1$ μm) grains (Horanyi & Mendis 1986c, Horanyi et al 1988). The authors have also discussed the hazards that these grains may pose to artificial satellites in or near geosynchronous orbit.

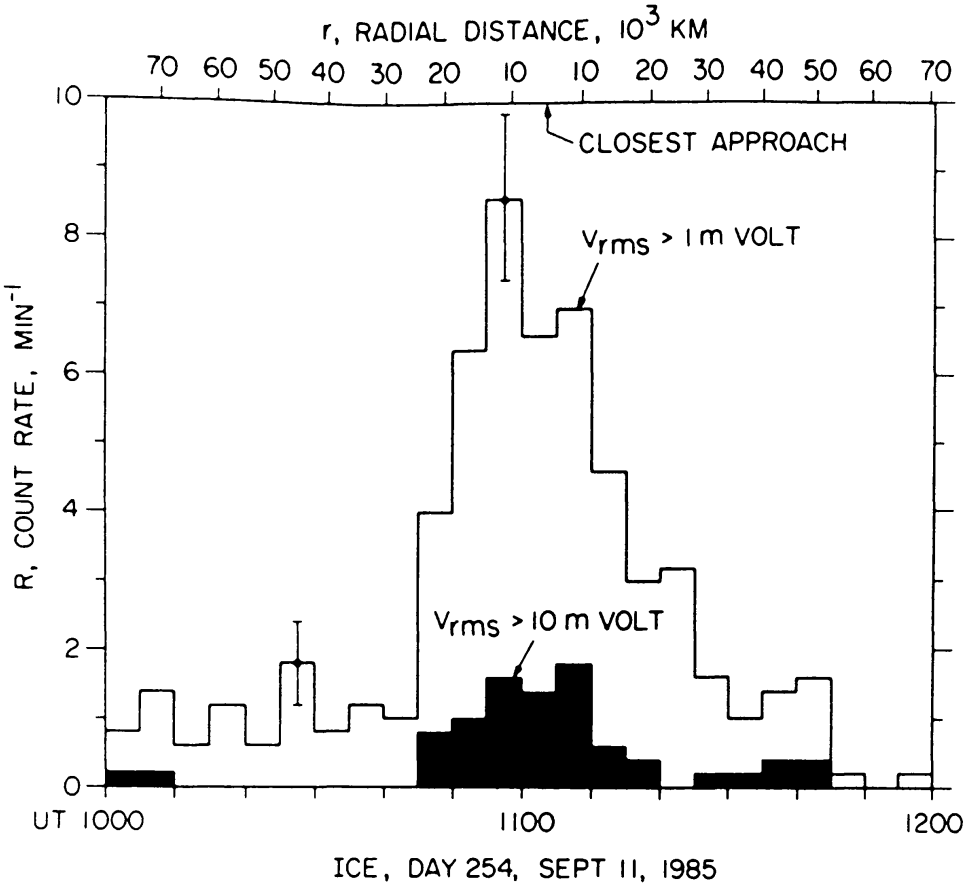

Figure 14 The counting rate for dust impacts exceeding two thresholds, 1 and 10 mVolt, measured by the *ICE* spacecraft. Most of the impacts occur within 30,000 km of closest approach to comet P/Giacobini-Zinner. Note that the amplitude of the voltage pulse (V_{rms}) is proportional to the grain mass. (From Gurnett et al 1986.)

5. WAVES, INSTABILITIES, AND WAVE SCATTERING

This section discusses collective effects in a dusty plasma as manifested by the behavior of waves and instabilities, and wave scattering on dust grains in a plasma. An early paper on the collective oscillations of a "microparticle plasma" used a multifluid model to study waves arising from a distribution of fluid velocities in a cold plasma comprised of a number of negatively and positively charged microparticles (James & Vermeulen 1968). As reviewed by Goertz (1989), several papers appeared on wave behavior in dusty astrophysical plasma in the 1980s, including studies of electrostatic dust beam-driven waves in Saturn's rings (Bliokh & Yarashenko 1985) and the effect of charged dust on Alfven wave propagation in interstellar clouds (Pilipp et al 1987). During the past few years there has been a substantial increase in theoretical studies of the collective behavior of dusty plasmas that address how the presence of charged dust grains in a plasma can affect wave dispersion properties, instabilities,

and wave scattering. We review some recent theoretical work in this rapidly developing, relatively new field of research.

5.1 *Waves*

When $a \ll d \ll \lambda_D$, the charged dust grains may be considered as point particles, similar to multiply-charged positive or negative ions (Fortov & Iakubov 1990). When the dust particles can be treated as just another component of the plasma, there are similarities with plasmas comprising electrons, ions, and additional negative (or positive) ions (D'Angelo 1990); however, there are differences from negative ion or two-ion component plasmas in several respects. First, typical dust grains have charge-to-mass ratios that are generally orders of magnitude smaller than those of ions. For example, a dust grain of mass density 0.5 gm/cm^2 and radius $a \sim 1$ micron has a mass of about 10^{12} proton masses; the charge $q_d = -Z_d e$ on such a grain in a thermal 10 eV oxygen plasma, when only plasma collection is considered, is of the order of $\sim 2.5 \times 10^4$ elementary electron charges. Since the plasma frequency of species α is $\omega_{p\alpha} = (4\pi n_\alpha q_\alpha^2/m_a)^{1/2}$ and the gyrofrequency of species α is $\Omega_\alpha = |q_\alpha B/m_\alpha c|$, typical frequencies associated with the dynamics of dust grains are very low compared with typical ion wave frequencies in standard electron-ion plasmas. Second, the grain charge depends on both the properties of the dust particles and the ambient plasma and radiative properties, as discussed in Section 2; thus the charge to mass ratio can differ in different environments even for a grain of fixed size and electrical properties. Third, it has been inferred or observed in situ that dust grains generally in space plasmas are polydisperse, that is, they have a size distribution, with the number density of grains generally given by a power law $n_d da \propto a^{-p} da$, with p ranging from ~ 0.9 to 4.5 in various space and astrophysical environments (e.g. Havnes 1990a and references therein). Since the dust mass $m_d \propto a^3$ and the dust charge q_d is generally $\propto a$ (see Section 2), the frequencies associated with the dust grains, such as the dust plasma frequency and the dust gyrofrequency, may be continuous variables (Goertz 1989).

Some basic properties of various waves in dusty plasmas have been obtained from multifluid analyses (e.g. Shukla 1992, D'Angelo 1990), which treat the dust grains as a component of a three-component plasma comprising electrons, ions, and (negatively or positively) charged dust of uniform mass and charge (and therefore of uniform size). The fluid equations for each species α are the equations of continuity and momentum,

$$\frac{\partial n_\alpha}{\partial t} = -\nabla \cdot (n_\alpha \mathbf{v}_\alpha) \tag{25}$$

$$n_\alpha m_\alpha \left(\frac{\partial}{\partial t} + \mathbf{v}_\alpha \cdot \nabla \right) \mathbf{v}_\alpha = -\nabla P_\alpha + q_\alpha n_\alpha \left(\mathbf{E} + \frac{\mathbf{v}_\alpha}{c} \times \mathbf{B} \right) \tag{26}$$

coupled with Maxwell's equations. In addition there is an equation expressing

overall charge neutrality in the plasma,

$$Z_i n_i + \varepsilon_d Z_d n_d = n_e \tag{27}$$

(where $\varepsilon_d = 1, -1$ for positively, negatively, charged grains respectively). Here q_α, Z_α are the charge, charge state of each species α, $\mathbf{E}$ and $\mathbf{B}$ are the electric and magnetic fields, and n_α, $\mathbf{v}_\alpha$, m_α, and P_α are the density, fluid velocity, mass, and (isotropic) pressure of each species α (α = e, i, d for electrons, ions, and dust grains, respectively) (e.g. Shukla 1992). To obtain dispersion relations for linear waves, the fluid equations are solved for small perturbations about an equilibrium steady state (denoted by subscript o), assuming that first-order quantities [denoted by superscript (1)] vary as $\exp[i(\mathbf{k}\cdot\mathbf{x} - \omega t)]$ (see e.g. Krall & Trivelpiece 1973). For electrostatic waves, $\mathbf{E}^{(1)} = -\nabla\phi^{(1)}$, where $\phi^{(1)}$ is the perturbed scalar potential, and $\mathbf{B}^{(1)} = \mathbf{0}$.

The presence of charged dust has been shown to both modify the usual linear modes known in an electron-ion plasma and lead to the presence of new modes associated with the dust grains in low frequency and low phase velocity regimes (e.g. Shukla 1992). For example, ion modes can be modified due to charge imbalance between the electrons and ions in the equilibrium state, that is, due to $n_{eo} \neq Z_i n_{io}$: Referring to the fluid equations, when the dust is assumed to be immobile (with the dust mass $m_d \to \infty$), the perturbed dust velocity $\mathbf{v}_d^{(1)} = 0$ from Equation (26) and dust contributes to the dispersion relation through the charge neutrality condition (27). New low-frequency modes associated with the response of the dust grains can arise when the dust grain dynamics are included via the momentum and continuity Equations (25 and 26) for the dust species.

In an unmagnetized dusty plasma, dust can modify the linear dispersion relation for ion-acoustic waves (Shukla & Silin 1992). In the phase velocity regime where electron inertia is negligible $v_{td}, v_{ti} \ll v_{ph} \ll v_{te}$ (where $v_{t\alpha}$ is the thermal speed of species α and $v_{ph} = \omega/k$), and in the limit of very large dust mass (e.g. considering the dust grains to be immobile) the dispersion relation for dust ion-acoustic waves in a plasma with electrons, singly-charged ions, and charged dust is (Shukla & Silin 1992)

$$\omega^2 = \delta \frac{k^2 c_s^2}{1 + k^2 \lambda_{De}^2}, \tag{28}$$

where $\delta = n_{io}/n_{eo} > 1$ for negatively charged dust, and $c_s = (k_B T_e/m_i)^{1/2}$ is the usual ion sound speed. Since the phase velocity of this mode for long wavelengths (i.e. $k\lambda_{De} \ll 1$) is $v_{ph} = (\delta k_B T_e/m_i)^{1/2}$, the dust ion-acoustic mode can exist as a normal mode of the system even for $T_e = T_i$ as long as dust grains carry most of the negative charge in the plasma, i.e. $\delta \gg 1$ [with $\delta < (m_i/m_e)$ in order to have $v_{ph} < v_{te}$], because in that case ion Landau damping is small. This is in contrast to the electron-ion plasma, where $T_e \gg T_i$ is required for propagation of ion-sound waves (Krall & Trivelpiece 1973).

This mode may be relevant in astrophysical situations where the plasma is isothermal but where dust can carry much of the negative charge, such as in the F -Ring of Saturn (Shukla & Silin 1992). This mode may also be relevant to the possible existence of an electrostatic shock just inside the ionopause of comet Halley. While observations of the ion density profile just inside the cometry ionopause are consistent with the existence of a shock (Damas & Mendis 1992), the exact nature of the shock is unclear. Körösmezey et al (1987) speculated on the existence of such an electrostatic shock due to the rapid increase in the calculated electron temperature just inside the ionopause. However, the values of T_e/T_i, calculated using different assumptions, are in the range ~2–5, which may not be sufficient to prevent Landau damping of the ion-acoustic wave which mediates the electrostatic shock. But the presence of a large quantity of dust, particularly in the form of VSGs, within the dusty cometary ionosphere may prevent this damping and allow such a shock to form.

In the lower phase velocity regime $v_{td} \ll v_{ph} \ll v_{ti}, v_{te}$ the presence of dust can lead to a new dust-acoustic wave associated with the grain dynamics (Rao et al 1990). Assuming that electron and ion inertia are negligible in this phase velocity regime (so that the left-hand side of Equation (26) = 0 for electrons and ions), and that the electrons and singly charged ions are in Boltzmann equilibrium, and also assuming that the dust fluid is cold and is described by Equations (25) and (26), the dispersion relation for the dust-acoustic wave was obtained as

$$\omega^2 = Z_d(\delta - 1)\frac{m_i}{m_d}\frac{k^2 c_s^2}{(1 + k^2\lambda_{De}^2 + \delta T_e/T_i)} \tag{29}$$

for negatively charged grains with $\delta > 1$. In this case, the electrons and ions provide the pressure while the dust mass provides the inertia (Rao et al 1990). Excitation of the dust-acoustic mode by streaming electrons and ions may have relevance to planetary rings, and is discussed in Section 5.2.

In a magnetized, homogeneous dusty plasma the presence of charged dust can similarly affect electrostatic waves such as acoustic waves, electrostatic ion cyclotron (EIC) waves, and lower hybrid waves. A multi-fluid analysis of a three-component dusty magnetized plasma (D'Angelo 1990) showed that there are two ion-acoustic waves and two EIC waves associated with the positive ions and the negative (or positive) dust grains. For negatively charged dust, frequencies of both acoustic waves increase with dust density [see also expressions (28) and (29)], as does the frequency of the positive ion EIC wave. For positively charged grains, the frequency of the ion acoustic mode decreases with increasing dust density, while the frequency of the ion EIC mode approaches the ion gyrofrequency as n_d increases. These results are shown in Figure 15: They are analogous to those obtained previously for either two-ion component (e.g. Suszcynsky et al 1989) or negative ion plasmas (e.g. D'Angelo et al 1966, Song et al 1989) apart from the different charge-to-mass ratio of the dust

(D'Angelo 1990). The dispersion relation of the lower hybrid mode in the frequency regime Ω_d, $\Omega_i \ll \omega \ll \Omega_e$, is also modified by the presence of charged dust: In the limit $m_d \to \infty$ in a dense plasma with $\omega_{pe}^2/\Omega_e^2 \gg 1$ (Shukla 1992), the lower hybrid wave frequency is

$$\omega^2 \approx \delta Z_i \Omega_e \Omega_i,$$

which increases as the negative dust density increases. We note that a cross-field current-driven lower hybrid instability has been invoked to provide anomalous resistivity in an electron-ion plasma in a protostellar cloud (Norman & Heyvaerts 1985). Since dust grains may carry most of the charge in the weakly ionized plasma of protostellar clouds during certain stages in their evolution (e.g. Nishi et al 1991, Umebayashi & Nakano 1990), the effect of dust on the lower hybrid instability may need to be examined.

The effect of negatively charged dust grains on electrostatic drift waves in an

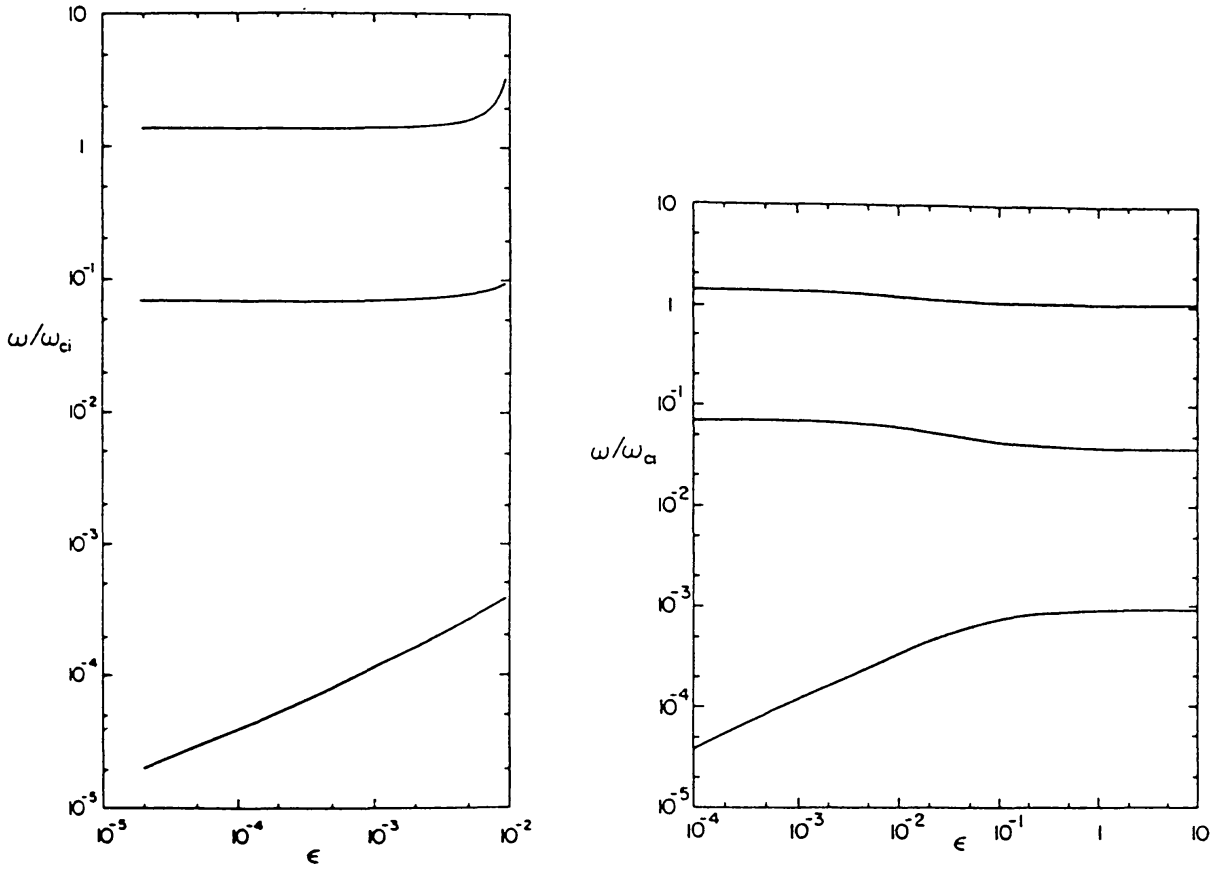

(a) (b)

Figure 15 (*a*) Wave frequency normalized to $\omega_{ci}(=\Omega_i)$ as a function of $\varepsilon = n_{do}/n_{io}$ for negatively charged grains. Here $m_d/m_i = 10^8$, $Z_d = 100$, $T_d/T_i = 0.1$, $T_i/T_e = 0.2$, $k_x\rho_i = 0.4$, and $k_z\rho_i = 0.04$, where $\mathbf{B} = (0, 0, B)$, $\mathbf{k} = (k_x, 0, k_z)$. (*b*) Same as (*a*), but for positively charged grains. (From D'Angelo 1990.)

inhomogeneous magnetized low $\beta(= 8\pi n_{io} k_B T/B^2)$ plasma was considered by Shukla et al (1991) using a multifluid analysis. The dynamics of negatively charged dust grains was shown to both modify the dispersion properties of the usual electrostatic drift waves, and lead to the appearance of new low frequency dust drift waves in the regime $\omega \ll \Omega_d$. In the latter case both the ions and the electrons are assumed to be in Boltzmann equilibrium, and a new drift wave appears which couples the dust drift and dust-acoustic waves (Shukla et al 1991).

Dust can also modify the dispersion properties of low frequency electromagnetic waves, including Alfven waves (Shukla 1992, Rao 1993) and magnetosonic waves (Rao 1993). For example, the Alfven wave spectrum in a cold plasma in the very low frequency regime $\omega \ll \Omega_d$ becomes (Shukla 1992)

$$\omega^2 = \frac{k^2 v_A^2}{[1 + (v_A/c)^2 + n_{do} m_d / n_{io} m_i]},$$

where the usual Alfven speed is $v_A = (B^2/4\pi n_{io} m_i)^{1/2}$. We note that for many astrophysical and space dusty plasmas, the last term in the denominator $n_{do} m_d / n_{io} m_i$ may be $\gg 1$ owing to the large ratio of the dust to ion mass [for example the ionized gas in cool, dense interstellar clouds e.g. Pilipp et al (1987)], so that the dust dynamics decreases the phase speed in this regime. Dust also leads to new branches of the dispersion curve in a cold plasma in analogy with negative ion plasmas (e.g. Teichmann 1966, Shawhan 1966). For example, for parallel (to **B**) propagation in a cold magnetized plasma with negatively charged grains, the right circularly polarized mode has a resonance at Ω_d and a cutoff at a higher frequency which depends on the fraction of charge density and mass density carried by the grains (Mendis & Rosenberg 1992, Shukla 1992). In addition, under certain conditions there can be whistler mode propagation for the left-handed circularly polarized mode in the regime $(\delta - 1)\Omega_i/\delta \gg \omega \gg \Omega_d$ (Mendis & Rosenberg 1992).

Nonlinear acoustic waves in dusty plasmas have also been investigated using multifluid analyses. Bharuthram & Shukla (1992) investigated the formation of large amplitude ion-acoustic solitons in a dusty unmagnetized plasma with negatively charged grains, cold ions, and Boltzmann distributed electrons. The presence of dust grains was found to lead to the appearance of rarefactive (negative potential) solitons, which do not exist in the absence of dust, as well as compressional (positive potential) solitons. Nonlinear ion-acoustic waves may be relevant to the formation of an electrostatic shock inside the ionopause at comet Halley, as discussed above in relation to the dust ion-acoustic wave. Rao et al (1990) showed that dust-acoustic waves could also propagate nonlinearly as solitons of either negative or positive potential in a three-component plasma with electrons, ion, and negatively charged, cold dust grains. Verheest (1992) extended the latter analysis to a multispecies dusty plasma, allowing for both

hot and cold electrons and for a number of cold dust grain species, and found also that both rarefactive and compressive solitons could propagate.

Other approaches have been used to study how charged dust grains affect waves in dusty plasmas in the regime $d \gtrsim \lambda_D$ (e.g. de Angelis et al 1988, 1989). Kinetic analyses have shown that dust can significantly affect wave propagation, even when the charge density carried by the grains is small compared with the electron or ion charge density, due to inhomogeneities arising from the dust grains and their screening clouds which modify the plasma equilibrium. De Angelis et al (1989) considered the parameter regime $|q_d n_{do}/e n_{eo}| \ll 1$ and showed that the presence of a random spatial distribution of charged, massive, fixed dust grains can modify the stationary equilibrium electron and ion distributions due to the dust-generated background electrostatic potential. Using a Vlasov analysis, it was shown that electron plasma waves could be damped in the "cold plasma" regime ($\omega \gg k v_{te}$), where Landau damping is negligible. This was interpreted as being due to the interaction of electrons with a low phase velocity wave ($\omega, \mathbf{k} - \mathbf{q}$), which resulted from the beating of an electron plasma wave characterized by ($\omega, \mathbf{k}$) with a zero-frequency wave (0, $\mathbf{q}$) arising from plasma density inhomogeneities around the charged grains. The wave damping rate was found to be of the order of $(q_d n_{do}/e n_{eo})^2 \omega_{pe}$ (de Angelis et al 1989). Following the method of de Angelis et al (1989), Salimullah & Sen (1992) investigated the low frequency response of a dusty plasma, finding both changes to the usual ion-acoustic wave and the appearance of a new mode with phase velocity $\ll v_{ti}$.

5.2 *Instabilities*

The presence of charged dust in a plasma can both modify the behavior of usual plasma instabilities and lead to the appearance of new instabilities. Since dust grains are subject to non-electromagnetic forces such as gravity, friction, or radiation pressure, there can be new sources of free energy to drive instabilities, including relative drifts between the charged dust and the lighter plasma particles (electrons and ions) in cosmic dusty plasma environments (e.g. Tsytovich et al 1990). In planetary rings for example, the dust grains, whose orbits are to first order Keplerian, move azimuthally around the planet with a speed between the Kepler and corotation speeds (see Section 4), while the plasma ions and electrons tend to corotate with the planet; this leads to a relative azimuthal drift between dust and plasma. Another example is in a dusty cometary environment, where there can be relative streaming between the dust and the solar wind plasma flow (Havnes 1988).

Several hydrodynamic and kinetic instabilities in dusty plasmas have been investigated. Havnes (1988; see also Hartquist et al 1992) used a kinetic analysis to study streaming instabilities in a cometary environment where there is a relative drift between the cometary dust and the solar wind plasma flow, with

flow speed u in the range $v_{te} > u > v_{ti}$. It was found that an instability driven by streaming dust in a three-component unmagnetized dusty plasma required small dust velocity dispersion and that the presence of a sufficiently high neutral density could quench the instability due to ion-neutral or electron-neutral collisions. The conditions for growth were found to be more probable for comets at large distances from the Sun. Two-stream instabilities driven by either ion or dust beams in an unmagnetized dusty plasma have also been studied by Bharuthram et al (1992), who found that the dust affects both growth rates and ranges of drift speeds for which instability occurs.

The Kelvin-Helmholtz instability can occur in a plasma when there is a gradient in the fluid flow speed between adjacent fluid layers, as happens for example in the cometary environment (e.g. Ershkovich & Mendis 1986). D'Angelo & Song (1990) considered the effect of either negatively or positively charged dust on the Kelvin-Helmholtz instability in a magnetized, low β plasma with shear in the ion field-aligned flow, using a multifluid analysis. The dust was assumed to be immobile and of uniform mass and charge. The charged dust alters the critical shear for the onset of instability from that in an electron-ion plasma, where a relative speed between adjacent flows of the order of the ion sound speed is required for instability (D'Angelo 1965). The critical shear increases with dust charge density in a plasma with negatively charged grains and decreases with dust charge density in a plasma with positively charged grains (D'Angelo & Song 1990).

Ion-acoustic and dust-acoustic instabilities were investigated using a standard Vlasov analysis for a dusty unmagnetized plasma with electrons, ions, and dust of uniform mass and charge (Rosenberg 1993). When the electrons have a weak drift u in a range $v_{ti} < u < v_{te}$, dust ion-acoustic waves can be excited if $\delta T_e/T_i \gg 1$ (in which case ion Landau damping is small), when u is greater than the phase velocity of the mode $\delta^{1/2}c_s$. This instability may be particularly relevant to cosmic plasmas, where generally it is assumed that $T_e \sim T_i$, in environments where dust carries much of the negative charge. For example, it has been shown that dust grains in weakly ionized plasmas in protostellar clouds may carry much of the negative charge by electron sticking during certain stages of cloud contraction (Umebayashi & Nakano 1990, Nishi et al 1991). Ion-acoustic instability in such a dusty plasma might lead to anomalous resistivity and anomalous magnetic field diffusion as contrasted with the case of isothermal electron-ion plasmas in protostellar clouds for which the instability may not be operative (Norman & Heyvaerts 1985).

The dust-acoustic mode may be excited under certain conditions when the plasma electrons and ions drift together with speed u relative to the charged dust component. For example, in planetary rings beyond the corotation radius, the dust grain azimuthal speed is controlled primarily by gravity, while the lighter plasma particles corotate with the planet [at Saturn's G Ring, which

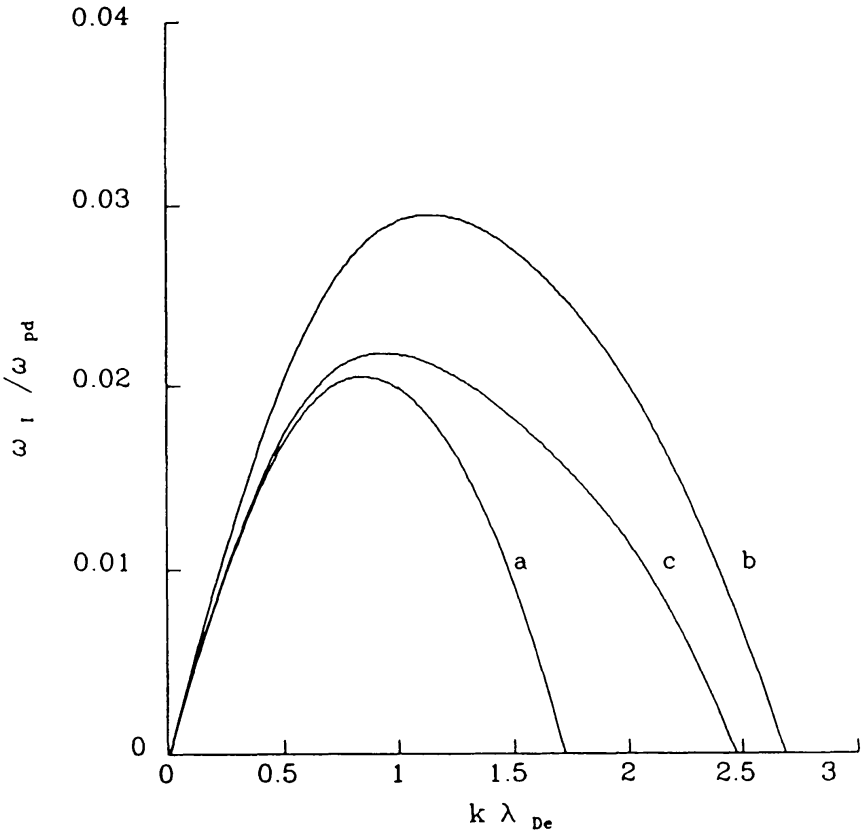

Figure 16 Growth rate of dust-acoustic instability ω_I normalized to dust plasma frequency ω_{pd} as a function of $k\lambda_{De}$ with $T_e = T_i = T_d$, $m_i/m_d = 1.6 \times 10^{-11}$, and $u/c_s = 0.2$. (*a*) $Z_d = 4 \times 10^4$, $n_{do}/n_{io} = 3 \times 10^{-8}$, $\varepsilon_d = -1$, (*b*) $Z_d = 10^2$, $n_{do}/n_{io} = 5 \times 10^{-3}$, $\varepsilon_d = -1$, (*c*) $Z_d = 10^3$, $n_{do}/n_{io} = 10^{-4}$, $\varepsilon_d = +1$. (From Mendis et al 1993.)

is located at about 2.8 radii from the planet, the Kepler speed is ~15 km/s, while the corotation speed is ~29 km/s (e.g. Mendis & Axford 1974); the ion thermal speed for oxygen in a 50 eV plasma is $v_i \sim 17$ km/s]. When the drift is weak ($v_{td} < u < v_{ti}$), dust-acoustic waves can be excited in the long wavelength limit ($k^2\lambda_{De}^2 < 1$) in an isothermal plasma if $R = Z_d|1-\delta|/(1+\delta) \gg 1$ (in which case dust Landau damping is small), when u is greater than the phase velocity of the mode $(Rm_i/m_d)^{1/2}c_s$. When $\delta \gtrsim 1$ (corresponding for example to dust parameters in the outer Saturnian rings) and the plasma is isothermal, the instability is driven primarily by the ions with maximum growth rate $\gamma \sim \sqrt{\pi/8}(u/c_s)\omega_{pd}$ (Rosenberg 1993). Growth rates for different values of Z_d and n_{do}/n_{io} are illustrated in Figure 16; the behavior with k is analogous to that of the usual ion-acoustic instability apart from the shift in k for maximum growth arising from the ion contribution to the effective Debye length. Typical dust plasma frequencies in the outer Saturnian rings, where $a \sim 1$ μm, $n_d \sim 3 \times 10^{-7}$ cm^{-3} (e.g. Goertz 1989), and the "isolated" grain charge value is $q_d \sim 5 \times 10^4$ elementary electron charges (assuming only plasma collection currents) yields an estimated dust plasma frequency, $\omega_{pd} \sim 0.04$ s^{-1}, which is large

compared with an ion-dust collision frequency $\tau_{id}^{-1} \sim \pi a^2 n_d v_{ti} \approx 10^{-7}$ s^{-1}, using values from Table 1. Melandsø et al (1993) have considered further the excitation of dust-acoustic waves including a model for wave damping by grain charge perturbations, and also found a regime of instability for parameters typical of Saturn's outer rings. Calculations that include the effect of the planetary magnetic field on these instabilities have yet to be done.

5.3 *Wave Scattering*

It has been shown that there can be enhanced wave scattering from dust grains in a plasma under certain conditions (e.g. Tsytovich et al 1989). Thomson scattering by dust grains, with a scattered power proportional to q_d^4/m_d^2, is negligible owing to the very large dust mass (Tsytovich 1992). However, an "isolated" charged dust grain in a plasma is surrounded by a cloud of plasma particles which screens out the grain charge over a distance of the order of a Debye length: For a negatively (positively) charged grain the screening cloud is comprised of both attracted ions (electrons) and repelled electrons (ions). A wave propagating through the plasma can be scattered coherently by the electrons in the screening cloud surrounding the charged grain when the wavelength is larger than the screening length. [The power scattered from the ions in the cloud would be smaller by a factor $\sim(m_e/m_i)^2$ (e.g. Tsytovich 1992, La Hoz 1992)]. This can lead to an increase in the scattering cross section as compared with scattering by free electrons or by fluctuations in the plasma (Tsytovich et al 1989; Bingham et al 1991, 1992; de Angelis et al 1992; La Hoz 1992; Hagfors 1992). When the scattering is coherent, all the electrons in the screening cloud move in phase, yielding a scattered power proportional to the square of the electron screening charge (Tsytovich 1992).

However, when n_d is large enough so that the grain charge (considering the contribution from plasma collection currents) is reduced due to the electron depletion effect, as discussed in Section 2.2, the enhancement decreases since there are fewer electrons in the screening cloud (de Angelis et al 1992). Calculations of electromagnetic wave scattering from charged dust particles in a plasma using "dressed test particle" approaches (La Hoz 1992, Hagfors 1992) found that for enhanced scattering d should be larger than a Debye length. In this case there is negligible electron depletion in the screening cloud surrounding the charged grain.

In the regime $d \gg \lambda_D \gg a$, each grain is screened in a distance of the order of the Debye length and the dust can be considered as a collection of individual scatterers (Bingham et al 1991). In this regime, for long incident wavelengths $\lambda_0 > d$, the scattering cross section for electromagnetic waves by dust grains is given by $\sigma = n_d \sigma_s$, where σ_s is the cross section for scattering from a single grain, which for $\lambda_0 \geq \lambda_D$ is given by $\sigma_s \simeq \sigma_0 Z_d^2$, where σ_0 is the Thomson cross section (Bingham et al 1991, 1992). Comparing this σ with the scattering cross

section from plasma fluctuations when no dust is present, $\sigma_p \simeq n_e \sigma_0/2$, implies that $n_d Z_d^2/n_e \gg 1$ is required for the scattering by "isolated" dust grains to dominate the scattering by plasma fluctuations (de Angelis et al 1992).

Havnes et al (1990b; see also Havnes et al 1992) suggested that the scattering from positively charged dust in the Earth's mesopause might explain the strong radar backscatter from the high latitude, summer mesopause observed at certain frequencies referred to as PSME (Polar Mesopheric Summer Echoes). The backscatter region occurs at an ionospheric height of about 80–90 km, which is also the altitude range of noctilucent clouds (e.g. Gadsden & Schröder 1989), which are thought to be comprised of solid particulates, probably mainly of ice (e.g. La Hoz 1992, Havnes et al 1990b). Havnes et al (1990b) suggest that if the photoelectric work function of mesospheric dust particles are lowered due to contaminants or impurities, the grains could attain surface potentials of a few volts positive even in the mesosphere where most of the solar photons have energy less than the photoelectric work function of amorphous ice. However, further work indicated that radar backscatter from dust particles may not fully explain PSME (La Hoz 1992, Hagfors 1992, Havnes et al 1992).

6. CONCLUSIONS

The study of cosmic dusty plasma is a relatively new area of research both with respect to theoretical development as well as specific applications. The study of the physics and dynamics of charged dust grains in certain solar system environments (discussed in Sections 3 and 4) arose in response to the observation (both in-situ and remote) of intriguing phenomena associated with fine dust. Here theory and observation continue to remain closely connected. While laboratory experimentation is lagging behind, recent experiments (e.g. Xu et al 1993) are beginning to clarify such basic questions as the relation of grain charge to the ratio d/λ_D, which had led to some early theoretical disagreements (e.g. see Goertz & Ip 1984, Whipple et al 1985).

The study of waves, instabilities, and scattering processes in dusty cosmic plasmas (discussed in Section 5) arose, however, not in response to specific observations, but from the realization that they are necessary consequences of dust-plasma interactions. As such this is an area where theory is leading observation. This is an area where theory is also leading experiment; at present we are unaware of any dedicated laboratory experiments on wave behavior in dusty plasmas [although observations of low frequency noise in a dust device were reported by Sheehan et al (1990)].

Waves associated with the presence of dust would not be directly observable in cosmic plasmas except perhaps via satellite observations in the solar system. Nonetheless they could have important ramifications that can be inferred. Wave turbulence generated by instabilities (discussed in Section 5) can lead

to anomalous resistivity and viscosity and associated anomalous transport processes. This would have implications for the macroscopic dynamics of certain cosmic environments. For example, if dust ion-acoustic waves can be excited in protostellar plasma clouds (see Section 5.2), then anomalous resistivity may play a role in the dissipation of magnetic fields in these clouds. This process of magnetic field decoupling from contracting cloud material is an outstanding issue in star formation scenerios (e.g. see Shu et al 1987). As another example, if a dust-acoustic instability is important in certain planetary rings (see Section 5.2), then the associated anomalous viscosity could have implication for the dynamics of dust grains in ring environments where the classical collisional drag between ions and grains appears to be unimportant (e.g. Mendis et al 1982).

We expect that as research in the area of dusty plasmas continue, it would stimulate further applications to phenomena in astrophysics and space science. The recent discovery of so-called VSGs in certain cosmic plasmas is an added impetus to these studies. Since these dust grains have large specific charges they would be most susceptible to electrodynamic forces. Furthermore, while they add negligibly to the dust/gas mass ratio, they significantly enhance the cummulative surface area of the dust in the plasma, which in turn would enhance the occurence of collective dusty-plasma processes.

ACKNOWLEDGMENTS

Support from the following grants are gratefully acknowledged: NASA NAGW-2252 and NSF AST-9213836 (M. R.); NASA NAGW-1502, NSF AST-9200981 and LANL/IGPP 93-132 (D. A. M.).

Literature Cited

Alfven H. 1954. *On the Origin of the Solar System,* p. 79. Oxford: Clavenden

Alfven H. 1980. *Cosmic Plasma.* Dordrecht:Reidel

Allen CW. 1983. *Astrophysical Quantities,* p. 160. London: Athlone. 3rd ed.

Armstrong TP, Paonessa MT, Bell, EV II, Krimigis SM. 1983. *J. Geophys. Res.* 88:8893

Bharuthram R, Saleem H, Shukla PK. 1992. *Phys. Scr.* 45:512

Bharuthram R, Shukla PK. 1992. *Planet. Space Sci.* 40:973

Bingham R, de Angelis U, Tsytovich VN, Havnes O. 1991. *Phys. Fluids* B3:811

Bingham R, de Angelis U, Tsytovich VN, Havnes O. 1992. *Phys. Fluids* B4:282

Bliokh PV, Yaroshenko VV. 1985. *Sov. Astron.* 29:330

Borderies N, Goldreich R, Tremaine S. 1984. In *Planetary Rings,* ed. R Greenberg, A Brahie, p. 713. Tucson: Univ. Ariz. Press

Burns JA, Schaffer LE, Greenberg RJ, Showalter MR. 1985. *Nature* 316:115

Chow VW, Mendis DA, Rosenberg M. 1993. *J. Geophys. Res.* 98:19065

Christon SP, Mitchell DG, Williams DJ, Frank L, Huang CY, Eastman TE. 1988. *J. Geophys. Res.* 97(E9):14,773

Connerney JEP, Waite JH. 1984. *Nature* 312:136

Consolmagno GJ. 1983. *J. Geophys. Res.* 88:5607

Cox DP, Reynolds RJ. 1987. *Annu. Rev. Astron.*

Astrophys. 25:303
Damas MC, Mendis DA. 1992 *Astrophys. J.* 396:704
D'Angelo N. 1965. *Phys. Fluids* 8:1748
D'Angelo N. 1990. *Planet. Space Sci.* 38:1143
D'Angelo N, Song B. 1990. *Planet. Space Sci.* 38:1577
D'Angelo N, von Goeler S, Ohe T. 1966. *Phys. Fluids* 9:1605
De Angelis U, Bingham R, Tsytovich VN. 1989. *J. Plasma Phys.* 42:445
De Angelis U, Forlani A, Tsytovich VN, Bingham R. 1992. *J. Geophys. Res.* 97:6261
De Angelis U, Formisano V, Giardano M. 1988. *J. Plasma Phys.* 40:399
Ershkovich AI, Mendis DA. 1986. *Astrophys. J.* 302:849
Fechtig H, Grun E, Morfill GE. 1979. *Planet. Space Sci.* 27:511
Feuerbacher B, Willis RF, Fitton B. 1973. *Astrophys. J.* 181:102
Flammer KR, Jackson B, Mendis DA. 1986. *Earth, Moon and Planets* 35:203
Fomenkova MN, Mendis DA. 1992. *Astrophys. Space Sci.* 189:327
Fortov VE, Iakubov IT. 1990. *Physics of Nonideal Plasma,* chap. 8. New York: Hemisphere
Gadsden M, Schröder W. 1989. *Noctilucent Clouds.* New York:Springer-Verlag
Goertz CK. 1989. *Res. Geophys.* 27:271
Goertz CK, Ip W-H. 1984. *Geophys. Res. Lett.* 11:349
Goertz CK, Morfill GE. 1983. *Icarus* 53:219
Gosling JT, Asbridge JR, Bame SJ, Feldman WC, Zwickl RD, et al. 1981. *J. Geophys. Res.* 86:547
Grun E, Morfill GE, Mendis DA. 1984. In *Planetary Rings,* ed. R Greenberg, A Brahick, p. 275. Tucson: Univ. Ariz. Press
Grun E, Morfill GE, Terrile RJ, Johnson TV, Schweln GT. 1983. *Icarus* 54:227
Gurnett DA, Averkamp TF, Scarf FL, Green E. 1986. *Geophys. Res. Letts.* 13:291
Hagfors T. 1992. *J. Atmos. Terr. Phys.* 54:333
Hartquist TW, Havnes O, Morfill GE. 1992. *Fundam. Cosmic. Phys.* 15:107
Havnes O. 1988. *Astron. Astrophys.* 193:309
Havnes O, Aanesen TK, Melandsø, F. 1990a. *J. Geophys. Res.* 95:6581
Havnes O, de Angelis U, Bingham R, Goertz CK, Morfill GE, Tsytovich V. 1990b. *J. Atmos. Terr. Phys.* 52:637
Havnes O, Goertz CK, Morfill GE, Grun E, Ip W-H. 1987. *J. Geophys. Res.* 92:2281
Havnes O, Melandsø F, La Hoz C, Aslaksen TK, Hartquist T. 1992. *Phys. Scr.* 45:535
Havnes O, Morfill GE, Goertz CK. 1984. *J. Geophys. Res.* 89:10999
Hill JR, Mendis DA. 1980a. *Can. J. Phys.* 59:897
Hill JR, Mendis DA. 1980b. *Moon and Planets* 23:53
Hill JR, Mendis DA. 1980c. *Astrophys. J.* 242:395
Hill JR, Mendis DA. 1982a. *J. Geophys. Res.* 87:7413
Hill JR, Mendis DA. 1982b. *Geophys. Res. Lett.* 9:1069
Hill JA, Mendis DA. 1982c. *Moon and Planets* 26:217
Horanyi M, Burns JA. 1991. *J. Geophys. Res.* 96:19,283
Horanyi M, Burns JA, Hamilton D. 1992. *Icarus* 97:248
Horanyi M, Burns JA, Tatrallyay M, Luhman JG. 1990. *Geophys. Res. Letts.* 17(6):853
Horanyi H, Goertz CK. 1990. *Astrophys. J.* 361:105
Horanyi M, Houpis HLF, Mendis DA. 1988. *Astrophys. Space Sci.* 144:215
Horanyi M, Mendis DA. 1986a. *Astrophys. J.* 307:800
Horanyi M, Mendis DA. 1986b. *J. Geophys. Res.* 91:335
Horanyi M, Mendis DA. 1986c. *Adv. Space Res.* 6(7):127
Horanyi M, Mendis DA. 1987. *Earth Moon and Planets* 35:203
Horanyi M, Morfill G, Grun E. 1993. *Nature* 363:1993
Horanyi M, Tatrallyay M, Juhaàsz A, Luhmann JG. 1991. *J. Geophys. Res.* 96:11,283
Houpis HLF, Mendis DA. 1983. *The Moon and Planets* 29:39
Intrilligator DS, Dryer M. 1991. *Nature* 353:407
Ip W-H. 1983. *J. Geophys. Res.* 88:819
Ip W-H, Mendis DA. 1983. *Geophys. Res. Letts.* 10:207
James CR, Vermeulen F. 1968. *Can. J. Phys.* 46:855
Jonker JH. 1952. *Phillips Res. Rep.* 7:1
Körösmezey A, Cravens TE, Gombosi TI, Nagy AF, Mendis DA, et al. 1987. *J. Geophys. Res.* 92:7331
Krall NA, Trivelpiece AW. 1973. *Principles of Plasma Physics.* New York:McGraw Hill
La Hoz C. 1992. *Phys. Scr.* 45:529
Laframboise JG, Parker LW. 1973. *Phys. Fluids* 16:629
Leubner MP. 1982. *J. Geophys. Res.* 87:6335
Lissauer JJ, Squyers SW, Hartman WK. 1988. *J. Geophys. Res.* 93:13776
Melandsø F, Aslaksen T, Havnes O. 1993. *J. Geophys. Res.* 98:13315
Mendis DA. 1981. In *Investigating the Universe,* ed. FD Kahn, p. 353. Dordrecht: Reidel
Mendis DA. 1991. *Astrophys. Space Sci.* 176:163
Mendis DA, Axford WI. 1974. *Rev. Earth Planet. Sci.* 2:419
Mendis DA, Hill JR, Houpis HLF, Whipple ECJ. 1981. *Astrophys. J.* 249:787
Mendis DA, Hill JR, Ip W-H, Goertz CK, Grun E, 1984. In *Saturn,* ed. T. Gehrels, MS Matthews, p. 54. Tucson: Univ. Ariz. Press

Mendis DA, Horanyi M. 1991. In *Cometary Plasma Processes,* ed. AJ Johnston, p. 17. Geophys. Monogr. No. 6. Washington, DC: AGU
Mendis DA, Houpis HLF, Hill JR. 1982. *J. Geophys. Res.* 87:3449
Mendis DA, Houpis HLF, Marconi ML. 1985. *Fundam. Cosmic. Phys.* 10:1
Mendis DA, Rosenberg M. 1992. *IEEE Trans. Plasma Sci.* 20:929
Mendis DA, Rosenberg M, Chow VV. 1993. In *Dusty Plasma, Noise and Chaos in Space and in the Laboratory,* ed. H. Kikuchi. New York: Plenum. In press
Meyer-Vernet N. 1982. *Astron. Astrophys.* 105:98
Morfill GE, Grun E, Johnson TV. 1980. *Planet. Space Sci.* 28:1087
Mueller AC, Kessler DJ. 1985. *Adv. Space Res.* 5(2):77
Nishi R, Nakano T, Umebayashi T. 1991. *Astrophys. J.* 368:181
Norman C, Heyvaerts J. 1985. *Astron. Astrophys.* 147:247
Northrop TG. 1992. *Physica Scr.* 45:475
Northrop TG, Birmingham. 1990. *Planet. Space Sci.* 38:319
Northrop TG, Connerney JEP. 1986. *Icarus* 70:124
Northrop TG, Hill JR. 1982. *J. Geophys. Res.* 87:6045
Northrop TG, Hill JR. 1983a. *J. Geophys. Res.* 83:1
Northrop TG, Hill JR. 1983b. *J. Geophys. Res.* 88:6102
Northrop TG, Mendis DA, Schaffer L. 1989. *Icarus* 79:101
Opik EJ. 1956. *Irish Astron. J.* 4:84
Pilipp W, Hartquist TW, Havnes O, Morfill GE, 1987. *Ap. J.* 314:341
Puget JL, Leger A. 1989. *Annu. Rev. Astron. Astrophys.* 27:161
Rao NN, Shukla PK, Yu MY. 1990. *Planet. Space Sci.* 38:543
Rao NN. 1993. *Planet. Space Sci.* 41:21
Raymond JC. 1984. *Annu. Rev. Astron. Astrophys.* 22:75
Rosenberg M. 1993. *Planet. Space Sci.* 41:229
Rosenberg M, Mendis DA. 1992. *J. Geophys. Res.* 97:14,773
Sagdeev RZ, Evlanov EN, Fomenkova MN, Prilutskii OF, Zubov BV. 1989. *Adv. Space. Sci.* 9:263
Salimullah M, Sen A. 1992. *Phys. Lett.* A 163:82
Sekanina Z, Farrell JA. 1980. In *Solid Particles in the Solar System,* ed. J. Halliday, BA McIntosh, p. 267. Dordrecht: Reidel
Shan, L-H, Goertz CK. 1991. *Astrophys. J.* 367:350
Shawhan SD. 1966. *J. Geophys. Res.* 71:5585
Sheehan DP, Carillo M, Heidbrink W. 1990. *Rev. Sci. Instrum.* 61:3871
Showalter MR, Burns JA, Cuzzi JN, Pollack JB, 1985. *Nature* 316:526
Shu FH, Adams FC, Lizano S. 1987. *Annu. Rev. Astron. Astrophys.* 25:23
Shukla PK. 1992. *Phys. Scr.* 45:504
Shukla PK, Silin VP. 1992. *Phys. Scr.* 45:508
Shukla PK, Yu MY, Bharuthram R. 1991. *J. Geophys. Res.* 96:21,343
Simpson JA, Rabinowitz D, Tuzzolino AJ, Ksanfomality LV, Sagdeev RZ. 1987. *Astron. Astrophys.* 187:742
Simpson JA, Tuzzolino AJ, Ksafomality LV, Sagdeev RZ, Vaisberg OL. 1989. *Adv. Space. Sci.* 9:259
Singer SF, Walker EH. 1962. *Icarus* 1:112
Smith BA, Soderblom LA, Beebe RF, Boyce J, Briggs GA, et al. 1982. *Science* 212:163
Song B, Suszcynsky D, D'Angelo N, Merlino RL. 1989. *Phys. Fluids* B1:2316
Spitzer L. 1941. *Astrophys. J.* 93:396
Stebbins J, Huffer CH, Whitford AE. 1934. *Publ. Washburn Obs.* 15:(V)
Stebbins J Huffer CH, Whitford AE. 1939. *Astrophys. J.* 90:209
Sternglass EJ. 1954. *Sci. Pap. 1772,* Westinghouse Res. Lab., Pittsburgh
Summers D, Thorne RM. 1991. *Phys. Fluids* 83:1835
Suszcynsky D, D'Angelo N, Merlino RL. 1989. *J. Geophys. Res.* 94:8966
Teichmann J. 1966. *Can. J. Phys.* 44:2973
Trumpler RJ. 1930. *Lick Obs. Bull.* 14:154
Tsytovich VN. 1992. *Phys. Scr.* 45:521
Tsytovich VN, de Angelis U, Bingham R. 1989. *J. Plasma Phys.* 42:429
Tsytovich VN, Morfill GE, Bingham R, De Angelis U. 1990. *Comments Plasma Phys. Controlled Fusion* 13:153
Umebayashi T, Nakano T. 1990. *MNRAS* 243:103
Verheest F. 1992. *Planet. Space Sci.* 40:1
Wallis MK, Hassan MHA. 1983. In *Cometary Exploration,* Vol. II, ed. TI Gombosi, p. 57. Budapest: Hungarian Acad. Sci.
Whipple EC Jr. 1965. *The equilibrium electric potential of a body in the upper atmosphere and in interplanetary space. NSASA-GSFC Publ. X-615-65-296*
Whipple EC Jr. 1981. *Rep. Prog. Phys.* 44:1197
Whipple EC Jr, Northrop TG, Mendis DA. 1985. *J. Geophys. Res.* 90:7405
Wilson GR. 1988. *J. Geophys. Res.* 93:12,771
Xu W, D'Angelo N, Merlino RL. 1993. *J. Geophys. Res.* 98:7843